DEVELOPMENT OF A GENETIC APPROACH TO STUDY INSULIN-DEGRADING ENZYME IN YEAST

by

SEONIL KIM

(Under the Direction of Walter K. Schmidt)

ABSTRACT

The Insulin-Degrading Enzyme (IDE) is a metalloprotease known for cleaving insulin and the neurotoxic amyloid beta peptide in humans. Because of these properties, IDE has been thought as having potential therapeutic value in Alzheimer disease. IDE has significant homology to yeast enzymes, Axl1p and Ste23p, which are important for production of the yeast **a**-factor mating pheromone. We have determined that yeast-expressed IDE can produce **a**-factor *in vivo* and cleave insulin *in vitro*. Accordingly, we conclude that IDE can be functionally expressed in yeast and propose that yeast can be used as a tractable model system to study the enzymatic function of IDE. This research aims to define the enzymatic properties of IDE, which could eventually lead to improved therapeutic approaches for the treatment of Alzheimer disease.

INDEX WORDS: Insulin-Degrading Enzyme, Alzheimer disease, Axl1p, Ste23p, Yeast mating, and **a**-factor mating pheromone

# DEVELOPMENT OF A GENETIC APPROACH TO STUDY INSULIN-DEGRADING ENZYME IN YEAST

by

SEONIL KIM

B.S., Chung-Ang University, Korea, 2003

A Thesis Submitted to the Graduate Faculty of The University of Georgia in Partial Fulfillment of the Requirements for the Degree

MASTER OF SCIENCE

ATHENS, GEORGIA

2005

# DEVELOPMENT OF A GENETIC APPROACH TO STUDY INSULIN-DEGRADING ENZYME IN YEAST

by

SEONIL KIM

Major Professor: Walter K. Schmidt

Committee: Jacek Gaertig
Michael Tiemeyer

Electronic Version Approved:

Maureen Grasso
Dean of the Graduate School
The University of Georgia
August 2005

ACKNOWLEDGEMENTS

I am grateful to those who helped all my works. First and foremost, I would like to express my sincere appreciation to my major advisor, Dr. Walter K. Schmidt for all his support and generosity over the last two years. I will remember him as a fine teacher, gentle advisor, and smart scientist, always.

Also, I want to thank the members of my committee, Drs. Jacek Gaertig and Michael Tiemeyer, for their support and advice. I appreciate the generosity of all lab members in the lab of Dr. Michelle Momany for use and help with their fluorescence microscope. Also, I thank Dr. Lance Wells and his lab members, especially, Jaemin and Dan, for their help with mass spectrometry.

I am really thankful to have worked with the past and present members of the Schmidt lab. Especially, I want to thank Andrea, Stephen, and Ben for their kind support. I learned a lot from these people, and they have always been good friends and colleagues.

Finally, I thank my family for their sincere love and support in my life and my wife for her love and patience. Also, I appreciate the kind advice of Won-jong. I would have never accomplished this work without all these people. I thank God.

TABLE OF CONTENTS

Page

# CHAPTER 1

# INTRODUCTION AND LITERATURE REVIEW

## 1.1. Alzheimer Disease (AD)

Alzheimer disease (AD) is a neurodegenerative disorder characterized by progressive memory loss. AD is currently the most common form of dementia in the elderly. The number of patients has continuously increased in the past several decades (1). Unfortunately, there is no definitive diagnostic test or therapy for this disease so far. There are two anatomical hallmarks in AD: extracellular deposits of amyloid beta peptides (Aβ) (2), and intracellular deposits of neurofibrillary tangles of tau proteins (3).

The Aβ peptide was first sequenced from the blood vessels of AD patients and people with Down's syndrome (2) and subsequently found in the senile plaques of AD patients brain tissue (4). These discoveries led to speculation that Aβ accumulation was a pathological important event in AD. Later, the presenilin proteins were found to be important for Aβ production (5). Mutation of APP and presenilins can stimulate production of amyloidogenic Aβ (6). Based on these observations, the amyloid hypothesis was developed, which states that the accumulation of Aβ is the underlying cause of AD pathogenesis (2). Testing this hypothesis has become the major focus of AD research.

The Aβ peptide is produced from the amyloid precursor protein (APP) by proteolytic cleavages mediated by the β- and γ-secretases. These cleavages affect the release of Aβ into the

extracellular space of cells in the cerebrum (7) (Fig. 1.1). Extracellular Aβ is cleared in a normal human brain by several mechanisms, including enzymatic degradation and receptor-mediated removal (8). The level of cerebral Aβ is presumed to be increased in AD patients, possibly because of an imbalance between the generation and clearance of Aβ (9). Decreased clearance and degradation of the Aβ peptide could be more common causes of AD than increased generation (8). In the clearance process, the low-density lipoprotein receptor-related protein (LRP) mediates the transport of Aβ from the brain across the Blood Brain Barrier (BBB) (10). Therefore, LRP has an important role in reducing Aβ burden in the brain. In the LRP-mediated export pathway, Aβ binds to α2-macroglobulin (α2M) or aplolipoprotein E (apoE) and forms a complex. These complexes bind to LRP, which are shuttled to the blood plasma where Aβ is removed (11). In the enzymatic degradation pathway, several proteases are reported to be involved. The Aβ peptide released in the cerebrum can undergo direct degradation by proteases. Neprilysin (NEP) and the insulin-degrading enzyme (IDE) are believed to be the major proteases involved in this process (12,13). While IDE only cleaves soluble and monomeric Aβ peptides, NEP can degrade an insoluble form of Aβ associated with membranes. Therefore, both NEP and IDE are likely to contribute independently to Aβ degradation in the brain (14).

Based on the amyloid hypothesis, the Aβ peptide is neurotoxic. Although there are no clear mechanisms to explain its neurotoxicity, several possibilities may explain Aβ toxicity. Some studies have suggested that oligomerization of the peptide is required for neurotoxicity (15). This oligomerized peptide triggers apoptosis through the p53 and Box pathways (16). Other studies suggest that oligomers could form ion channels, which lead to inappropriate membrane depolarization, apoptosis involving Box and Bcl-2 proteins, and release of toxic lysosomal

contents that ultimately cause neurodegeneration (17). Third, the Aβ peptide could interact with mitochondria in the neuron of AD patients and induce apoptosis and oxidative damage through the interaction of Aβ and Aβ-binding alcohol dehydrogenase (ABAD) (18). Another hypothesis explaining Aβ toxicity is that inflammation generated by microglia around Aβ deposit plaques induces neurodegeneration (19). Despite the several possible mechanisms proposed to explain Aβ toxicity, the exact process has not been determined.

Several therapeutic approaches have been proposed for the treatment of AD (Fig. 1.2). One approach is based on the observation that Aβ generation depends on the activity of β- and γ-secretases. Therefore, therapies are being developed to inhibit secretases. However, these enzymes are involved in other functions, such as Notch signaling (20,21). Thus, there is a need to develop inhibitors that are selective for APP processing. A second approach targets Aβ oligomerization. After Aβ is released, oligomerization is believed to be an important first step toward neurotoxicity. Therefore, disrupting fibrillogenesis is considered a potential therapy to prevent Aβ toxicity. Metals such as zinc (Zn) and copper (Cu) can modulate Aβ oligomerization (22). Thus, Cu/Zn chelators have been developed to disrupt Aβ fibrillar formation (23). A third potential therapy is based on blocking Aβ transport into the brain by Aβ vaccination. An anti-Aβ antibody has been described that retains Aβ in the plasma and prevents it from transporting back into the brain (24). Another treatment against AD may be vaccination against the insoluble aggregating peptides. In transgenic animal models, immunization can prevent the formation of amyloid deposits as well as learning deficits (25). Anti-inflammatory drugs have also been shown to decrease the level of Aβ in various cell lines and to reduce inflammation, oxidative damage and plaque formation in the animal AD model (26,27). One anti-inflammatory drug directly interacts with γ-secretase to reduce the cleavage of APP (26).

Enhancing the activity of proteases that directly degrade Aβ such as IDE and NEP represents a novel therapeutic approach. However, this strategy will require a way to selectively increase the enzymatic activity toward Aβ so as to avoid cleaving other substrates of these enzymes, such as insulin and endorphins (8).

### 1.2. The linkage between diabetes and AD

Diabetes is known to increase the risk of development of AD (28). There are several possibilities to explain the linkage between diabetes and AD. First, advanced glycation end-products (AGEs) are sugar-modified proteins that are resistant to protease degradation and accumulate in both diabetes and AD (29). AGEs stimulate oxidative stress, which is believed to be toxic to cells (30). Second, Tau phosphorylation and neurofibrillary tangle formation are increased in both diseases through disruption of the insulin signaling (31). Third, Aβ aggregation is increased by inhibition of IDE activity which is responsible for the control of insulin and Aβ levels (32). Other recently published reports support a linkage between IDE and type 2 diabetes (33). These include the observation that *IDE* gene maps to a region on chromosome 10 that is associated with type 2 diabetes (34,35). In addition, mutations of IDE result in a decrease insulin degradation and induce other diabetes-related phenotypes (36). IDE also cleaves amylin, the major component of pancreatic islet amyloid that is a hallmark of type 2 diabetes (37). Although the relationship between the two diseases is not still understood, the development of diabetes and AD may be connected via insulin metabolism and IDE activity.

### 1.3. Insulin-Degrading Enzyme (IDE)

IDE was first proposed to be responsible for insulin proteolysis *in vivo* (38). Several observations support a role for IDE in insulin proteolysis. First, degraded insulin products are found in cells expressing IDE. Second, injection of an anti-IDE antibody inhibits cellular

degradation of insulin. Third, inhibitors of IDE, such as N-ethylmaleimide (NEM), inhibit insulin degradation. Finally, insulin can be crosslinked to IDE in cells (36,39).

IDE has been purified from several mammalian tissues, including red blood cells, skeletal muscle, liver, and brain (36). Purified IDE has a mass of 110 kDa on denaturating polyacrylamide gels. Under nondenaturing conditions, IDE is reported to exist as a dimer or tetramer (40). IDE is a member of the M16A metalloprotease family. These enzymes require zinc and are highly conserved from *Escherichia coli* to human (41). For example, human IDE shares 22% amino-acid sequence identity with *Saccharomyces cerevisiae* Axl1p (41), 27% with *E. coli* protease III (42), 48% with *Drosophila melanogaster* IDE (43), and 95% with rat IDE (44). These proteases have the same zinc-binding site involved in catalysis, -His-Xaa-Xaa-Glu-His- (HxxEH) (36). Mutation of any one of these conserved amino acids inactivates the protease (45-47). Based on the high level of sequence conservation, we hypothesize that M16A family proteases may have similar substrate specificity. As mentioned above, IDE is a zinc-dependent metalloprotease. Not surprisingly, IDE is sensitive to chelating agents such as 1, 10-phenanthroline. In addition, it is inhibited by sulfhydryl-modifying reagents such as NEM. Therefore, a sulfhydryl group in IDE has been proposed to be required for its activity. This sulfhydryl group may be necessary for maintaining an active conformation of the enzyme rather than being directly involved in catalytic activity (36).

Most IDE is found in cytosolic fractions (39), but small amounts of the protein are associated with other subcellular fractions, including plasma membranes, endosomes, and peroxisomes (36). IDE has a canonical peroxisomal targeting motif, -Ala/Ser-Lys-Leu- (A/SKL), that purportedly localizes it to peroxisomes (48). However, IDE does not have to be in

peroxisome to be active (49). The multiple cellular locations of IDE suggest multifunction roles for the enzyme *in vivo* (36).

In addition to insulin, IDE degrades several other peptides which can form or are predicted to form amyloid fibrils. These include the amyloid beta peptide (13), atrial natriuretic peptide (ANP) (50), amylin (37), calcitonin (51), yeast **a**-factor mating pheromone (52) among others (Table 1.1). The specificity of a protease is usually determined by amino acids located at or near a cleavage site. However, there is no significant sequence similarity between the cleavage site of the various substrates of IDE, although IDE appears to exhibit a preference for basic (Arg) or large hydrophobic (Phe, Leu, Tyr) amino acids near the cleavage site (39,53). These observations suggest that IDE may recognize substrates by secondary or tertiary structure instead of primary sequence (54). Although there is no definitive structural similarity between substrates, they all appear to have the ability to form, under certain conditions, amyloid fibrils (55). Therefore, these data suggest that IDE may have a role for clearance of amyloid-forming peptides.

### 1.4. The Role of IDE in AD

Based on the amyolid hypothesis, the clearance of Aβ is important for avoiding neurotoxicity. Several pieces of evidence support the role of IDE in the Aβ clearance. First, IDE is one of the major enzymes responsible for the degrading process (14). Second, the *IDE* gene is one of several candidate genes located in chromosome 10 that is linked to AD susceptibility (1). However, the most convincing evidence has come from IDE knockout mice. The endogenous levels of Aβ in the brain of knockout mice of IDE are increased, 1.5-fold. In addition, heterozygous *IDE-/+* mice show Aβ levels that are intermediate between wild-type and homozygous knockout mice, and primary neuronal cultures from knockout mice have less Aβ

degrading activity *in vitro* (33,56). In another study, levels of soluble and insoluble Aβ are 50% decreased in APP/IDE double transgenic mice. Also, Aβ plaques are reduced by 50%, and there is significant decrease of premature death in this animal model (57). These findings support an important role for IDE in Aβ degradation and suggest that IDE activity has responsibility for controlling Aβ levels *in vivo*.

### 1.5. M16A Metalloproteases in *Saccharomyces cerevisiae* (Axl1p and Ste23p)

The budding yeast *Saccharomyces cerevisiae* is a unicellular eukaryote that can exist stably as a haploid or diploid. Haploids are one of two mating types, *MAT***a** and *MAT*α. These haploid cells have the ability to divide mitotically or to mate with the opposite mating type to form the diploid (Fig. 1.3). Mating in yeast is mediated by the pheromones, **a**-factor and α-factor, produced by *MAT***a** and *MAT*α haploid cells, respectively. The production of **a**-factor requires the activity of Axl1p and Ste23p (Fig. 1.4). These yeast enzymes are members of M16A metalloprotease family. In addition, they have significant sequence similarity to IDE and share the same catalytic motif (HxxEH) (58).

Axl1p has several previously described functions. These include the regulation of the axial budding pattern (41), **a**-factor production (58), cell fusion during yeast mating (59), and haploid invasive growth (60). Axl1p was first found as a determinant of the haploid budding pattern. Yeast cells choose their bud site in a specific pattern that depends on cell type: axial for haploid cells and bipolar for diploid cells (61). *AXL1* is expressed in haploids but not diploids, and ectopic expression of *AXL1* in diploid cells induces change of the bipolar budding pattern to an axial pattern (41). In addition, Axl1p localizes to the mother-bud neck and division region and colocalizes with Bud3p, Bud4p, and Bud10p, which are proteins required for axial budding (62). This localization suggests that Axl1p is an important molecule for regulating haploid budding

pattern along with other structural proteins (62). Interestingly, the role of Axl1p in selecting the budding pattern does not require its proteolytic activity (58). Therefore, Axl1p is possibly a bi-functional enzyme.

In addition to its role in bud site selection, Axl1p has an independent role in yeast mating (58). It is required for production of the **a**-factor mating pheromone. The two **a**-factor genes, *MFA1* and *MFA2*, encode precursor peptide of 36 and 38 amino acids, respectively. These precursors contain an N-terminal extension and C-terminal CAAX motif (C is cysteine, A is aliphatic, and X can be any amino acid) (63). Many eukaryotic proteins such as the Ras proteins have the CAAX motif, which is a signal for posttranslational modifications, including farnesylation of the cysteine residue, C-terminal proteolysis, and methylation of the cleaved C-terminus (64).

Ax1lp also represses haploid invasive growth. Under glucose starvation, haploid cells switch a growth form from axial budding form to a filamentous form. The ability to switch growth form is required for three modifications: cells are elongated, cells attach to each other, bipolar budding pattern is maintained (60). These changes cause haploid invasive growth. It requires maintaining the bipolar budding pattern. As mentioned above, Axl1p maintains the axial budding pattern and is regulated by glucose availability. Therefore, Axl1p plays a role as a repressor in haploid invasive growth.

Ste23p is also a member of the M16A metalloprotease family. It is expressed in both haploid and diploid yeast cells (unpublished observation). It has a partial overlapping function with Axl1p in promoting the second N-terminal cleavage associated with **a**-factor production. Unlike Ax1lp, Ste23p is not responsible for maintaining the axial budding pattern (58). Its roles in invasive growth and other yeast physiological functions have not been previously investigated.

## 1.6. Methods for study of IDE activity

IDE has an important role in clearance of Aβ in AD and is therefore a promising therapeutic target. Several methods to evaluate the activity of IDE have been previously reported. The standard method is an *in vitro* insulin degradation assay using trichloracetic acid (TCA) (36). In spite of its widespread use, the TCA assay is not sensitive as compared to an established HPLC assay (65). Novel *in vitro* assays have been recently reported that utilize fluorogenic peptide substrates (53,66). The substrate specificity and kinetics of IDE have been investigated through these novel substrates. However, there is still limitation of *in vitro* assays. For example, *in vitro* assays usually ignore unknown regulators, activators, or inhibitors of reactions, which could exist in biological systems. To overcome this limitation, people suggest *in vivo* models such as genetically modified animals. Mice genetic models to study IDE functions have been created, which are knockout of IDE or transgenic mice overexpressing IDE (33,56,57). Phenotypes of these animal models support a role of IDE in Aβ degradation *in vivo*. However, these genetic models also have time and budget problems when working with animals. Therefore, novel model systems are still needed for the study of IDE function *in vivo*. This thesis reports the development of yeast as a model system for the study of IDE.

## 1.7. Summary and hypothesis

Alzheimer disease is characterized by progressive memory loss. This observation is thought to be mediated by the neurotoxic Aβ peptide. An imbalance between Aβ production and degradation is proposed to cause neurodegeneration. Therefore, the clearance of Aβ is important for preventing neurotoxicity. IDE is a metalloprotease that is involved in this Aβ clearance process. Thus, it should be considered as a potential therapeutic target for AD. The yeast enzymes Axl1p and Ste23p are related to IDE. These proteases have the same zinc-binding

motif (HxxEH) and are likely to have similar proteolytic activity. In this study, we hypothesize that IDE can substitute for the biological functions of Axl1p and Ste23p, and these M16A metalloproteases can all cleave amyloid forming peptides. Our findings suggest that yeast can be used as a genetic model system to study IDE as well as other M16A metalloproteases, and we also expect that our yeast genetic system will prove to be a novel method to overcome the limitations of previously described *in vitro* assays and *in vivo* model systems.

## 1.8. References


1. Tanzi, R. E., and Bertram, L. (2005) *Cell* **120**(4), 545-555
2. Glenner, G. G., and Wong, C. W. (1984) *Biochem Biophys Res Commun* **122**(3), 1131-1135
3. Wood, J. G., Mirra, S. S., Pollock, N. J., and Binder, L. I. (1986) *Proc Natl Acad Sci U S A* **83**(11), 4040-4043
4. Masters, C. L., Simms, G., Weinman, N. A., Multhaup, G., McDonald, B. L., and Beyreuther, K. (1985) *Proc Natl Acad Sci U S A* **82**(12), 4245-4249
5. Levy-Lahad, E., Wasco, W., Poorkaj, P., Romano, D. M., Oshima, J., Pettingell, W. H., Yu, C. E., Jondro, P. D., Schmidt, S. D., Wang, K., and et al. (1995) *Science* **269**(5226), 973-977
6. Scheuner, D., Eckman, C., Jensen, M., Song, X., Citron, M., Suzuki, N., Bird, T. D., Hardy, J., Hutton, M., Kukull, W., Larson, E., Levy-Lahad, E., Viitanen, M., Peskind, E., Poorkaj, P., Schellenberg, G., Tanzi, R., Wasco, W., Lannfelt, L., Selkoe, D., and Younkin, S. (1996) *Nat Med* **2**(8), 864-870
7. Selkoe, D. J. (1998) *Trends Cell Biol* **8**(11), 447-453
8. Tanzi, R. E., Moir, R. D., and Wagner, S. L. (2004) *Neuron* **43**(5), 605-608
9. Hardy, J., and Selkoe, D. J. (2002) *Science* **297**(5580), 353-356
10. Zlokovic, B. V. (2004) *J Neurochem* **89**(4), 807-811
11. Herz, J. (2003) *J Clin Invest* **112**(10), 1483-1485
12. Howell, S., Nalbantoglu, J., and Crine, P. (1995) *Peptides* **16**(4), 647-652
13. Kurochkin, I. V., and Goto, S. (1994) *FEBS Lett* **345**(1), 33-37
14. Selkoe, D. J. (2001) *Neuron* **32**(2), 177-180

15. Geula, C., Wu, C. K., Saroff, D., Lorenzo, A., Yuan, M., and Yankner, B. A. (1998) *Nat Med* **4**(7), 827-831

16. Zhang, Y., McLaughlin, R., Goodyer, C., and LeBlanc, A. (2002) *J Cell Biol* **156**(3), 519-529

17. Kagan, B. L., Hirakura, Y., Azimov, R., Azimova, R., and Lin, M. C. (2002) *Peptides* **23**(7), 1311-1315

18. Lustbader, J. W., Cirilli, M., Lin, C., Xu, H. W., Takuma, K., Wang, N., Caspersen, C., Chen, X., Pollak, S., Chaney, M., Trinchese, F., Liu, S., Gunn-Moore, F., Lue, L. F., Walker, D. G., Kuppusamy, P., Zewier, Z. L., Arancio, O., Stern, D., Yan, S. S., and Wu, H. (2004) *Science* **304**(5669), 448-452

19. Bamberger, M. E., and Landreth, G. E. (2001) *Microsc Res Tech* **54**(2), 59-70

20. De Strooper, B., and Konig, G. (1999) *Nature* **402**(6761), 471-472

21. Saura, C. A., Choi, S. Y., Beglopoulos, V., Malkani, S., Zhang, D., Shankaranarayana Rao, B. S., Chattarji, S., Kelleher, R. J., 3rd, Kandel, E. R., Duff, K., Kirkwood, A., and Shen, J. (2004) *Neuron* **42**(1), 23-36

22. Bush, A. I., Pettingell, W. H., Multhaup, G., d Paradis, M., Vonsattel, J. P., Gusella, J. F., Beyreuther, K., Masters, C. L., and Tanzi, R. E. (1994) *Science* **265**(5177), 1464-1467

23. Cherny, R. A., Atwood, C. S., Xilinas, M. E., Gray, D. N., Jones, W. D., McLean, C. A., Barnham, K. J., Volitakis, I., Fraser, F. W., Kim, Y., Huang, X., Goldstein, L. E., Moir, R. D., Lim, J. T., Beyreuther, K., Zheng, H., Tanzi, R. E., Masters, C. L., and Bush, A. I. (2001) *Neuron* **30**(3), 665-676

24. DeMattos, R. B., Bales, K. R., Cummins, D. J., Paul, S. M., and Holtzman, D. M. (2002) *Science* **295**(5563), 2264-2267

25. Schenk, D., Barbour, R., Dunn, W., Gordon, G., Grajeda, H., Guido, T., Hu, K., Huang, J., Johnson-Wood, K., Khan, K., Kholodenko, D., Lee, M., Liao, Z., Lieberburg, I., Motter, R., Mutter, L., Soriano, F., Shopp, G., Vasquez, N., Vandevert, C., Walker, S., Wogulis, M., Yednock, T., Games, D., and Seubert, P. (1999) *Nature* **400**(6740), 173-177

26. Weggen, S., Eriksen, J. L., Das, P., Sagi, S. A., Wang, R., Pietrzik, C. U., Findlay, K. A., Smith, T. E., Murphy, M. P., Bulter, T., Kang, D. E., Marquez-Sterling, N., Golde, T. E., and Koo, E. H. (2001) *Nature* **414**(6860), 212-216

27. Lim, G. P., Chu, T., Yang, F., Beech, W., Frautschy, S. A., and Cole, G. M. (2001) *J Neurosci* **21**(21), 8370-8377

28. Ott, A., Stolk, R. P., Hofman, A., van Harskamp, F., Grobbee, D. E., and Breteler, M. M. (1996) *Diabetologia* **39**(11), 1392-1397

29. Munch, G., Thome, J., Foley, P., Schinzel, R., and Riederer, P. (1997) *Brain Res Brain Res Rev* **23**(1-2), 134-143

30. Gasic-Milenkovic, J., Loske, C., and Munch, G. (2003) *J Alzheimers Dis* **5**(1), 25-30

31. Schubert, M., Brazil, D. P., Burks, D. J., Kushner, J. A., Ye, J., Flint, C. L., Farhang-Fallah, J., Dikkes, P., Warot, X. M., Rio, C., Corfas, G., and White, M. F. (2003) *J Neurosci* **23**(18), 7084-7092

32. Watson, G. S., Peskind, E. R., Asthana, S., Purganan, K., Wait, C., Chapman, D., Schwartz, M. W., Plymate, S., and Craft, S. (2003) *Neurology* **60**(12), 1899-1903

33. Farris, W., Mansourian, S., Chang, Y., Lindsley, L., Eckman, E. A., Frosch, M. P., Eckman, C. B., Tanzi, R. E., Selkoe, D. J., and Guenette, S. (2003) *Proc Natl Acad Sci U S A* **100**(7), 4162-4167

34. Myers, A., Holmans, P., Marshall, H., Kwon, J., Meyer, D., Ramic, D., Shears, S., Booth, J., DeVrieze, F. W., Crook, R., Hamshere, M., Abraham, R., Tunstall, N., Rice, F., Carty, S., Lillystone, S., Kehoe, P., Rudrasingham, V., Jones, L., Lovestone, S., Perez-Tur, J., Williams, J., Owen, M. J., Hardy, J., and Goate, A. M. (2000) *Science* **290**(5500), 2304-2305

35. Ertekin-Taner, N., Graff-Radford, N., Younkin, L. H., Eckman, C., Adamson, J., Schaid, D. J., Blangero, J., Hutton, M., and Younkin, S. G. (2001) *Genet Epidemiol* **21**(1), 19-30

36. Duckworth, W. C., Bennett, R. G., and Hamel, F. G. (1998) *Endocr Rev* **19**(5), 608-624

37. Bennett, R. G., Duckworth, W. C., and Hamel, F. G. (2000) *J Biol Chem* **275**(47), 36621-36625

38. Mirsky IA, B.-K. R. (1949) *Arch Biochem* **20**, 1-9

39. Authier, F., Posner, B. I., and Bergeron, J. J. (1996) *Clin Invest Med* **19**(3), 149-160

40. Song, E. S., Juliano, M. A., Juliano, L., and Hersh, L. B. (2003) *J Biol Chem* **278**(50), 49789-49794

41. Fujita, A., Oka, C., Arikawa, Y., Katagai, T., Tonouchi, A., Kuhara, S., and Misumi, Y. (1994) *Nature* **372**(6506), 567-570

42. Cheng, Y. S., and Zipser, D. (1979) *J Biol Chem* **254**(11), 4698-4706

43. Kuo, W. L., Gehm, B. D., and Rosner, M. R. (1990) *Mol Endocrinol* **4**(10), 1580-1591

44. Baumeister, H., Muller, D., Rehbein, M., and Richter, D. (1993) *FEBS Lett* **317**(3), 250-254

45. Gehm, B. D., Kuo, W. L., Perlman, R. K., and Rosner, M. R. (1993) *J Biol Chem* **268**(11), 7943-7948

46. Perlman, R. K., Gehm, B. D., Kuo, W. L., and Rosner, M. R. (1993) *J Biol Chem* **268**(29), 21538-21544

47. Perlman, R. K., and Rosner, M. R. (1994) *J Biol Chem* **269**(52), 33140-33145

48. Authier, F., Rachubinski, R. A., Posner, B. I., and Bergeron, J. J. (1994) *J Biol Chem* **269**(4), 3010-3016

49. Chesneau, V., Perlman, R. K., Li, W., Keller, G. A., and Rosner, M. R. (1997) *Endocrinology* **138**(8), 3444-3451

50. Muller, D., Baumeister, H., Buck, F., and Richter, D. (1991) *Eur J Biochem* **202**(2), 285-292

51. Kirschner, R. J., and Goldberg, A. L. (1983) *J Biol Chem* **258**(2), 967-976

52. Kim, S., Lapham, A. N., Freedman, C. G., Reed, T. L., and Schmidt, W. K. (2005) *J Biol Chem*

53. Song, E. S., Mukherjee, A., Juliano, M. A., Pyrek, J. S., Goodman, J. P., Jr., Juliano, L., and Hersh, L. B. (2001) *J Biol Chem* **276**(2), 1152-1155

54. Kurochkin, I. V. (2001) *Trends Biochem Sci* **26**(7), 421-425

55. Kurochkin, I. V. (1998) *FEBS Lett* **427**(2), 153-156

56. Miller, B. C., Eckman, E. A., Sambamurti, K., Dobbs, N., Chow, K. M., Eckman, C. B., Hersh, L. B., and Thiele, D. L. (2003) *Proc Natl Acad Sci U S A* **100**(10), 6221-6226

57. Leissring, M. A., Farris, W., Chang, A. Y., Walsh, D. M., Wu, X., Sun, X., Frosch, M. P., and Selkoe, D. J. (2003) *Neuron* **40**(6), 1087-1093

58. Adames, N., Blundell, K., Ashby, M. N., and Boone, C. (1995) *Science* **270**(5235), 464-467

59. Elia, L., and Marsh, L. (1998) *J Cell Biol* **142**(6), 1473-1485

60. Cullen, P. J., and Sprague, G. F., Jr. (2002) *Mol Biol Cell* **13**(9), 2990-3004

61. Chant, J., and Pringle, J. R. (1995) *J Cell Biol* **129**(3), 751-765

62. Lord, M., Inose, F., Hiroko, T., Hata, T., Fujita, A., and Chant, J. (2002) *Curr Biol* **12**(15), 1347-1352

63. Michaelis, S., and Herskowitz, I. (1988) *Mol Cell Biol* **8**(3), 1309-1318

64. Chen, P., Sapperstein, S. K., Choi, J. D., and Michaelis, S. (1997) *J Cell Biol* **136**(2), 251-269

65. Frank, B. H., Peavy, D. E., Hooker, C. S., and Duckworth, W. C. (1983) *Diabetes* **32**(8), 705-711

66. Leissring, M. A., Lu, A., Condron, M. M., Teplow, D. B., Stein, R. L., Farris, W., and Selkoe, D. J. (2003) *J Biol Chem* **278**(39), 37314-37320

**Table 1.1.** *Peptide substrates of IDE that form amyloid fibrils in humans* (modified from (54)).

| Amyloid protein | Length (aa) | Disease or involved tissue | Cleaved by IDE |
|---|---|---|---|
| Amyloid beta | 40-43 | Alzheimer disease | + |
| Atrial natriuretic peptide | 28 | Cardiac atria | + |
| Amylin | 37 | Type 2 diabetes | + |
| Insulin | A chain – 21<br>B chain – 30 | Diabetes | + |
| Calcitonin | 32 | Medullary carcinoma of the thyroid | + |
| Abri | 34 | Familial British dementia | ND |
| Medin | 50 | Aortic medial amyloid | ND |
| Yeast **a**-factor[a] | 12 | ND | + |

[a] The formation of amyloid fibrils of **a**-factor has not been established.

**Fig. 1.1.** *The proteolytic processing of APP and the fate of Aβ.*

Amyloid precursor protein (APP) is a membrane-bound protein that is cleaved by β- and γ-secretases to produce amyloid beta peptide (Aβ). The Aβ peptide is released in the extracellular space and undergoes oligomerization to form oligomers, which later generate plaques.

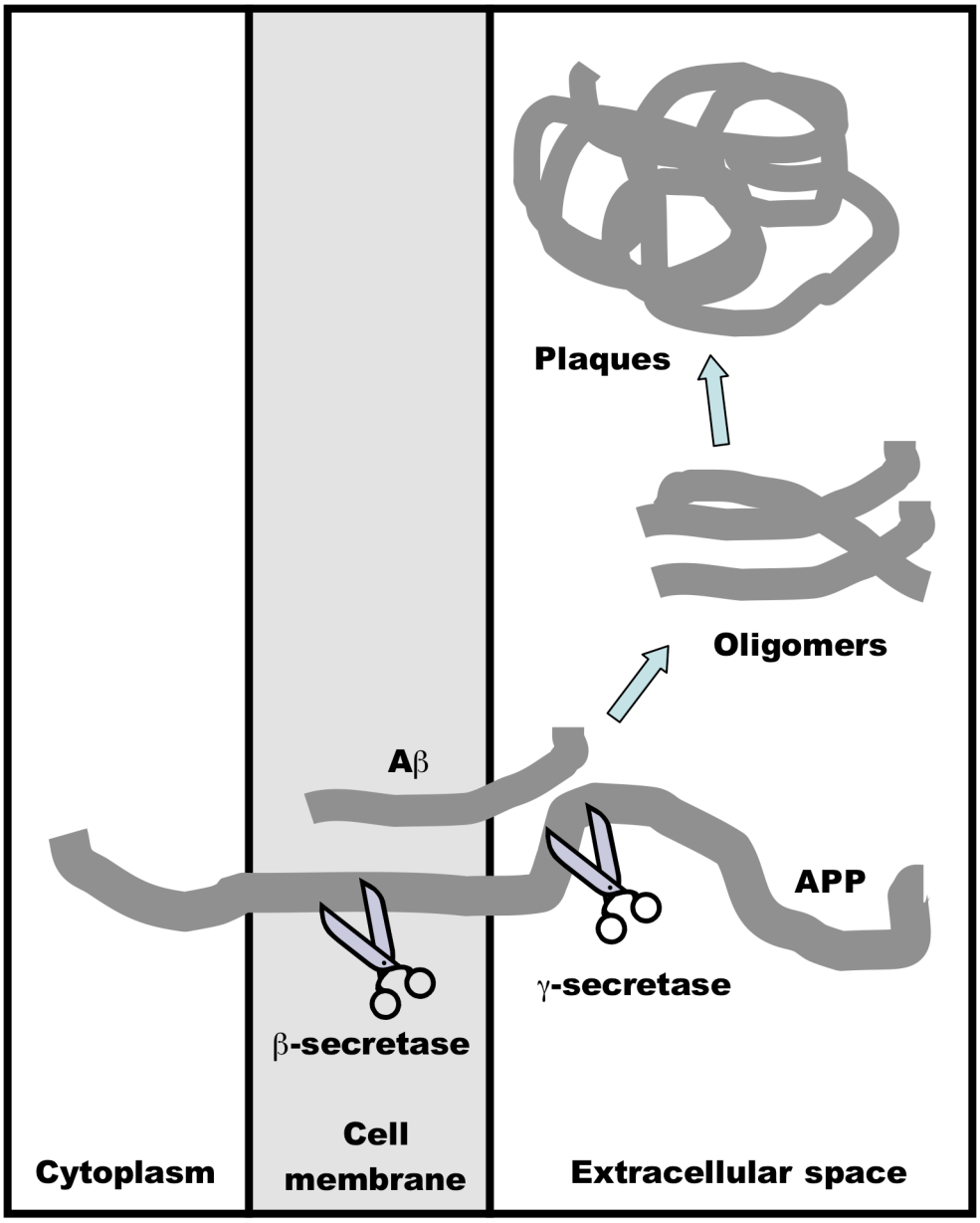
Plaques
Oligomers
Aβ
APP
γ-secretase
β-secretase
Cytoplasm
Cell membrane
Extracellular space

**Fig. 1.2.** *The Aβ life cycle and possible points of therapeutic approaches.*

Aβ production depends on the activity of β- and γ-secreteases cleaving APP. To prevent Aβ production, development of β- and γ-secretease inhibitors is a potential therapeutic approach. After Aβ is released, metals such as zinc and copper can induce Aβ oligomerization which is believed to induce neurotoxicity. Therefore, chealators can be applied to inhibit oligomerization. In addition, the Aβ peptide forms a complex with apoE, α2M and LRP. This complex is transported to the plasma where it is degraded. However, Aβ sometimes undergoes re-entry into the brain. Aβ vaccine will block this transport and increase peripheral degradation of Aβ. Another anti-Aβ antibody produced through Aβ vaccination can prevent the plaque formation. Finally, Aβ can be directly degraded by protease such as IDE and NEP. Therefore, these enzymes can be considered as therapeutic agents.

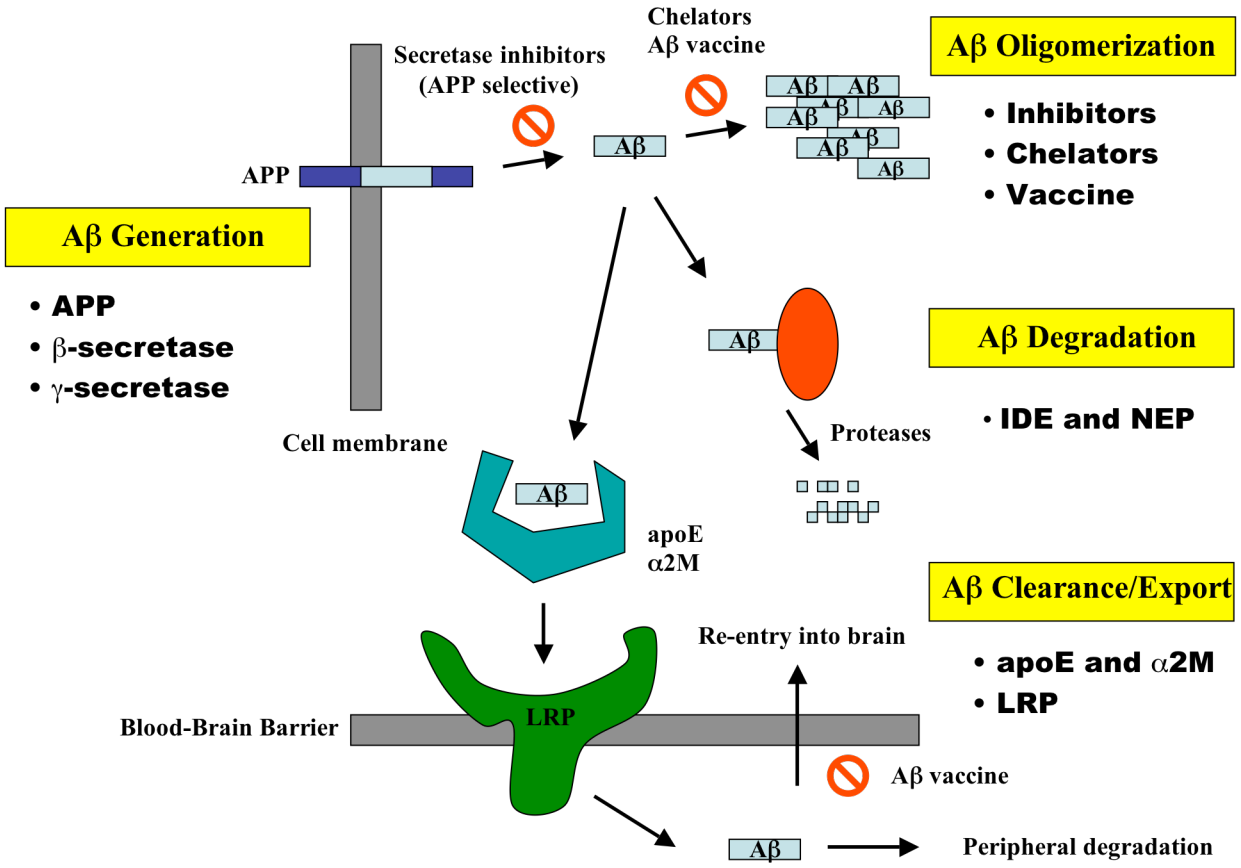
Chelators
Aβ vaccine
Secretase inhibitors
(APP selective)
Aβ Oligomerization
• Inhibitors
• Chelators
• Vaccine
APP
Aβ Generation
• APP
• β-secretase
• γ-secretase
Aβ
Aβ Degradation
• IDE and NEP
Proteases
Cell membrane
apoE
α2M
Aβ Clearance/Export
• apoE and α2M
• LRP
Re-entry into brain
Blood-Brain Barrier
LRP
Aβ vaccine
Peripheral degradation

**Fig. 1.3.** *The life cycle of S. cerevisiae*.

All three cell types of yeast, haploid *MAT***a**, *MAT*α, and diploid are able to proliferate and undergo mitotic division. The mating of haploids generates a diploid cell, and meiosis regenerates the haploid. Mating is dependent on mating pheromones, **a**-factor and α-factor secreted by *MAT***a** and *MAT*α cells, respectively. Under nutritional starvation, diploid cells undergo sporulation and meiosis to form a tetrad including two *MAT***a** cells and two *MAT*α cells, which are encased in a spore coat. The spores germinate and grow in a nutritional rich condition.

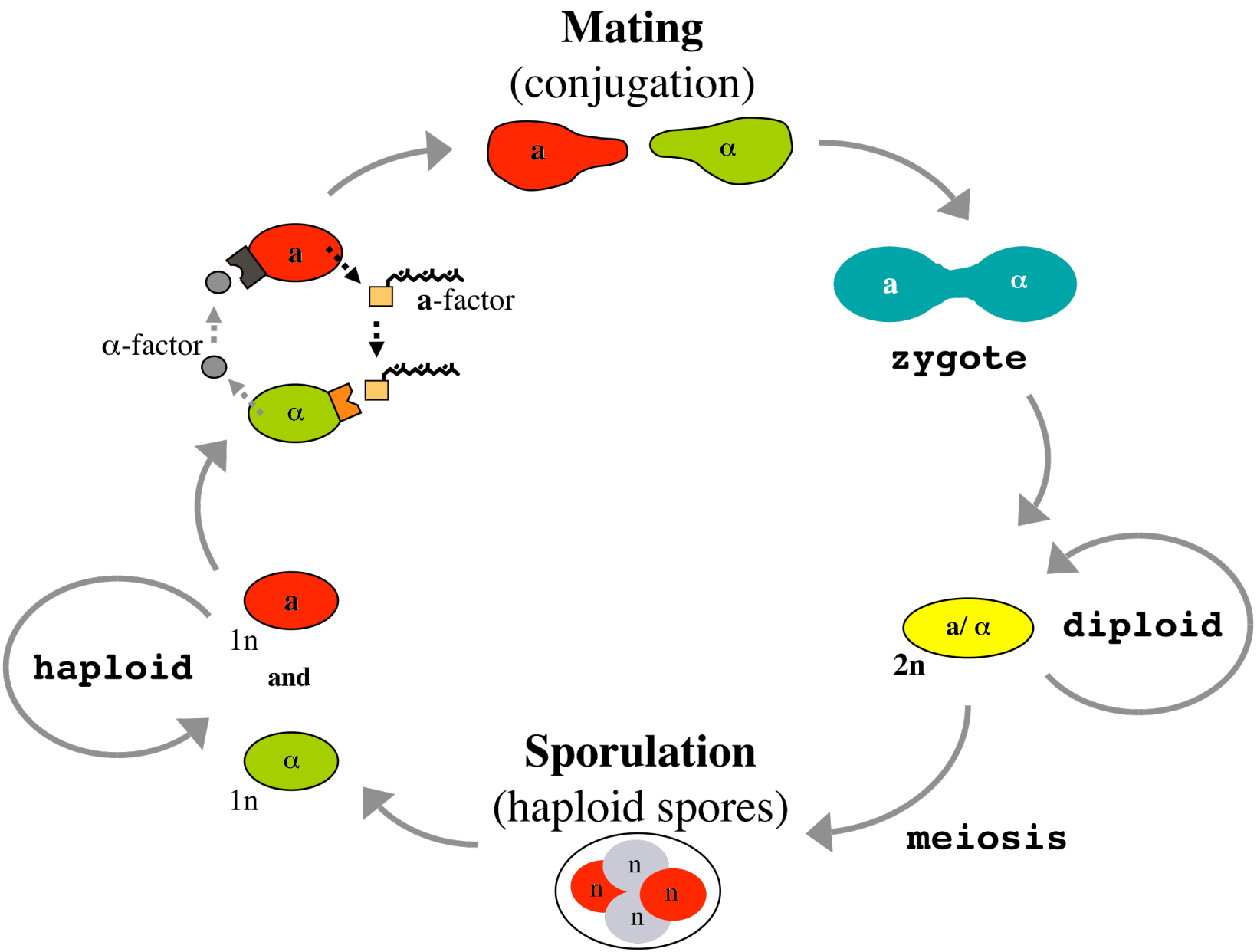
Mating
(conjugation)
a
α
a
α
zygote
a/ α
2n
diploid
meiosis
Sporulation
(haploid spores)
n
n
n
n
a
1n
and
α
1n
haploid
a
α
a-factor
α-factor

**Fig. 1.4.** *The biogenesis of the yeast **a**-factor mating pheromone.*

The yeast **a**-factor mating pheromone is a farnesylated and carboxylmethylated peptide secreted from haploid *MAT***a** cells. The pheromone is produced through several post-translational modifications. The **a**-factor precursor (P0) is encoded by the *MFA1* or *MFA2* genes (the *MFA1* precursor is shown). The CaaX motif in the precursor signals for C-terminal modifications: farnesylation, C-terminal cleavage, and carboxylmethylation (Steps 1-3). These steps require: Ram1p and Ram2p (farnesylation), Rce1p or Ste24p (CaaX proteolysis), and Ste14p (methylation). After CaaX modifications, the **a**-factor intermediate (P1) undergoes two sequential proteolysis at its N-terminus (Steps 4-5). Ste24p is required for the first cleavage, and Axl1p or Ste23p are responsible for the second proteolysis. These modifications yield mature **a**-factor (M). Finally, the mature pheromone is exported by the ABC transporter Ste6p (Step 6).

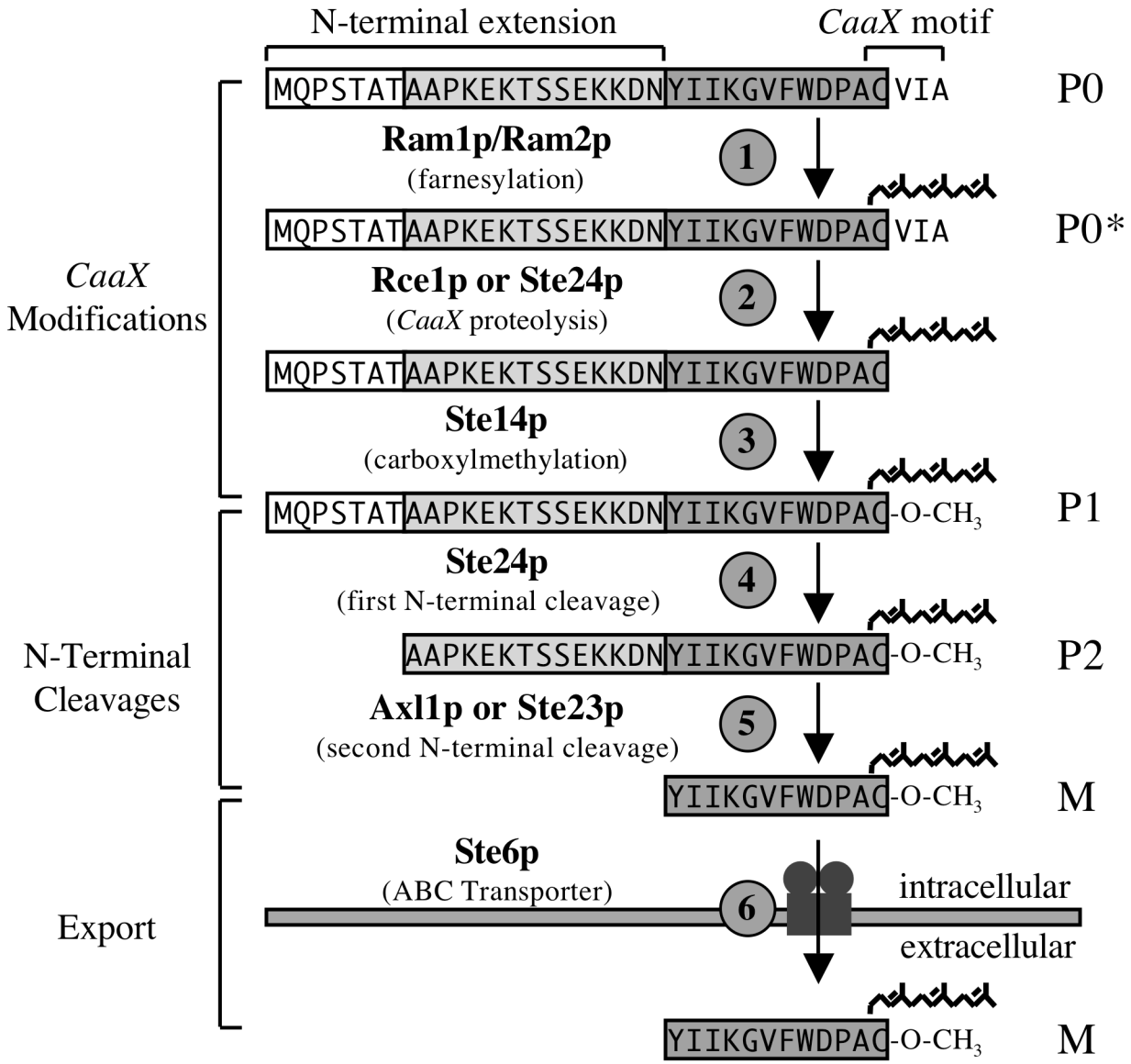
N-terminal extension
CaaX motif
MQPSTATAAPKEKTSSEKKDNYIIKGVFWDPACVIA
P0
Ram1p/Ram2p
(farnesylation)
1
MQPSTATAAPKEKTSSEKKDNYIIKGVFWDPACVIA
P0*
CaaX
Modifications
Rce1p or Ste24p
(CaaX proteolysis)
2
MQPSTATAAPKEKTSSEKKDNYIIKGVFWDPAC
Ste14p
(carboxylmethylation)
3
MQPSTATAAPKEKTSSEKKDNYIIKGVFWDPAC-O-CH3
P1
Ste24p
(first N-terminal cleavage)
4
N-Terminal
Cleavages
AAPKEKTSSEKKDNYIIKGVFWDPAC-O-CH3
P2
Axl1p or Ste23p
(second N-terminal cleavage)
5
YIIKGVFWDPAC-O-CH3
M
Ste6p
(ABC Transporter)
6
intracellular
Export
extracellular
YIIKGVFWDPAC-O-CH3
M

# CHAPTER 2

# YEAST AS A TRACATABLE GENETIC SYSTEM FOR FUNCTIONAL STUDIES OF THE INSULIN-DEGRADING ENZYME[1]

[1] Seonil Kim, Andrea N. Lapham, Christopher G. K. Freedman, Tiffany L. Reed, and Walter K. Schmidt. 2005. *The Journal of Biological Chemistry*. 280 (30):27481-27490
Reprinted here with permission of publisher

## ABSTRACT

We have developed yeast as an expression and genetic system for functional studies of the insulin-degrading enzyme (IDE), which cleaves and inactivates certain small peptide molecules, including insulin and the neurotoxic Aβ peptide. We show that heterologously expressed rat IDE is enzymatically active, as judged by the ability of IDE-containing yeast extracts to cleave insulin *in vitro*. We also show that IDE can promote the *in vivo* production of the yeast **a**-factor mating pheromone, a function normally attributed to the yeast enzymes Axl1p and Ste23p. However, IDE cannot substitute for the function of Axl1p in promoting haploid axial budding and repressing haploid invasive growth, activities that require an uncharacterized activity of Axl1p. Particulate fractions enriched for Axl1p or Ste23p are incapable of cleaving insulin, suggesting that the functional conservation of these enzymes may not be bidirectionally conserved. We have made practical use of our genetic system to confirm that residues comprising the extended zinc-metalloprotease motif of M16A family enzymes are required for the enzymatic activity of IDE, Ste23p, and Axl1p. We have determined that IDE and Axl1p both require an intact C-terminus for optimal activity. We expect that the tractable genetic system that we have developed will be useful for investigating the enzymatic and structure/function properties of IDE, and possibly for the identification of novel IDE alleles having altered substrate specificity.

## INTRODUCTION

The insulin-degrading enzyme (IDE; EC 3.4.24.56) has broad substrate specificity, being able to cleave and inactivate a number of small molecules, including the Aβ peptides and insulin (1-3). In animal models, IDE-deficiency correlates with increased levels of insulin and Aβ, and increased risks of type 2 diabetes and Alzheimer disease (4-6). Despite these and other findings, the biological role of IDE and its importance in the clearance of insulin and Aβ remains to be fully clarified (7).

The Ste23p and Axl1p proteins from *Saccharomyces cerevisiae* have significant sequence homology to IDE (36% and 19% identity, respectively) (8). Genetic and mutational studies indicate that Ste23p and Axl1p are required for the proteolytic maturation of the yeast **a**-factor mating pheromone, a lipid-modified peptide that is produced by a multi-step process (9,10). This pheromone is produced by *MAT***a** haploid cells and is required for yeast mating, the fusion of *MAT***a** and *MAT*α haploid cells to form a diploid cell. Although Ste23p and Axl1p can independently promote **a**-factor maturation, the enzymes are not fully redundant. Ste23p is significantly less efficient than Axl1p at producing biologically active pheromone (9).

Axl1p has several cellular roles. In addition to its role in pheromone production, Axl1p is required for the efficient post-conjugation fusion of haploid mating partners (11). This role may be indirectly related to the ability of Axl1p to produce **a**-factor, since limiting levels of pheromone similarly leads to fusion defects (12). Axl1p is also required for maintenance of the axial budding pattern that is characteristic of haploid yeast (8,9). In the absence of Axl1p, haploid yeast exhibit a bipolar budding pattern that is typical of diploid cells. The function of Axl1p in this process does not require its proteolytic activity, suggesting that Axl1p is a bi-functional enzyme (9). Axl1p also represses the invasive growth of haploid yeast (13,14).

Whether the proteolytic, bud site selection, or another activity of Axl1p is required for this process has not been reported. By contrast to Axl1p, the only reported cellular role for Ste23p is in **a**-factor production. Additional functions for this enzyme are likely since Ste23p is expressed in both the *MAT*α and diploid cell types that do not produce **a**-factor.[2]

IDE, Ste23p, and Axl1p are members of the M16A protease subfamily. M16A proteases are characterized by a core inverted zinc metalloprotease motif that is typically located within the first 200 residues of these enzymes and a pair of glutamic acid residues that are 70 and 77 amino acids distal to the core motif (*i.e.*, $HxxEHx_{69}Ex_6E$). The spacing between the core motif and the distal glutamates is invariant for all forty-six M16A enzymes so far identified, except in the case of Axl1p where the spacing is 76 residues. The histidine residues and most distal glutamate residue are putative zinc ligands, and mutational alteration of these residues inactivates IDE and Axl1p (9,15,16). Some members of the M16A subfamily, including IDE, are sensitive to thiol modifiers, suggesting that a cysteine residue(s) is critical for proper structure of the active site or the overall tertiary or quaternary structure of these proteins (1,15). Sequence alignment of IDE and its yeast orthologs reveals two conserved cysteine residues. One is within the core metalloprotease motif, and this residue can reportedly be altered without affecting enzymatic activity (15). The other conserved cysteine is exactly 67 amino acids distal to the extended motif ($HxxEHx_{69}Ex_6Ex_{67}C$). This distal cysteine is not conserved in *E. coli* Protease III, a bacterial M16A enzyme that is insensitive to thiol modifiers (17).

The sequence similarity between IDE, Ste23p, and Axl1p has prompted us to investigate the hypothesis that these proteins have conserved enzymatic properties and substrate specificity. To this end, we present evidence indicating that rat IDE can substitute for Axl1p and Ste23p in **a**-

[2] unpublished observation

factor production, but not for the other known functions of Axl1p. Importantly, these findings establish yeast as a genetically tractable system for future studies of IDE function. We have made practical use of this system to create and characterize novel mutations that alter the enzymatic properties of IDE.

## EXPERIMENTAL PROCEDURES

***Strains and Media*** **-** The yeast strains used in this study are listed in Table 2.1. Plasmid-bearing versions of these strains were generated by transformation with the indicated plasmids according to published methods (18). Strains were routinely grown at 30 °C on synthetic complete dropout (SC-) media, as previously described (19).

***Plasmids*** **-** The plasmids used in this study are indicated in Table 2.2. Plasmids p80 (*CEN URA3 AXL1*) and p137 (*CEN URA3 STE23*) have been previously described and were kindly provided by Dr. C. Boone (University of Toronto) (9). The other plasmids used in this study were created by PCR-directed recombination-mediated plasmid construction and/or standard molecular methods (20).

The general strategy for the epitope tagging of *AXL1*, *STE23* and *IDE* encoding plasmids involved the creation of a novel restriction site at the end of the respective ORF and subcloning of a triply iterated HA tag. pWS371 (*CEN URA3 AXL1-2HA*) was created by modifying p80 as follows. An *NcoI* site was inserted immediately prior to the stop codon of *AXL1* into which a DNA fragment encoding a triply iterated HA tag was inserted; in actuality, two tandem copies of the tag were inserted. The plasmid was further modified to delete a portion of the 5' untranslated region corresponding to an *XhoI* fragment in order to reduce the overall size of this plasmid from

12.1 to 10.6 kb; this deletion had no effect on protein expression. pWS482 (*CEN URA3 STE23-2HA*) was created by modifying p137 in a similar manner to that described for p80. In this instance, a *BamHI* site was introduced immediately prior to the stop codon of *STE23* into which a triply iterated HA tag was inserted; as with pWS371, two tandem copies of the tag were actually inserted. pWS511 (2$\mu$ *URA3* $P_{PGK}$*-IDE-HA*) was created by PCR amplification of IDE from pSR$\alpha$-rat IDE such that the PCR product had ends homologous to the parent yeast vector (pSM703) and a *BglII* restriction site immediately before the stop codon of IDE (21). The *BglII* site was used for insertion of the triply iterated HA epitope tag. pWS496 is identical to pWS511 except that it contains two copies of the triply iterated HA tag. Restriction digest analysis and DNA sequencing were used to confirm the presence of the tag in each of the plasmids described above.

The general strategy for the creation of site directed mutations in the above plasmids also involved PCR-directed recombination-mediated plasmid construction. In brief, a DNA fragment encoding an appropriate segment of the target ORF was amplified by PCR where one of the oligonucleotides contained the mutation of interest and typically a silent restriction site. The DNA fragments were co-transformed with a target plasmid that had been linearized or gapped with restriction enzymes near the intended site of mutation. Recombinant plasmids were recovered from yeast, amplified in *E. coli*, and screened by restriction analysis and/or sequencing to verify the presence of the mutation. All mutant alleles were confirmed by immunoblot to encode full-length protein.

The epitope tagging of Ste23p was not straightforward. DNA sequencing of an intermediate plasmid in the construction pWS482 revealed an extra nucleotide near the 3' end of the open reading frame (ORF) that was not present in the public sequence of *STE23*. The presence of the

extra nucleotide was confirmed in the *STE23* sequence derived from three different sources: p137 and PCR products derived from chromosomal amplification of the *STE23* gene from two distinct strain backgrounds (IH1783 and YPH499). An independent group has recently proposed the identical sequence annotation as part of an effort to identify mistakes in published genome sequences (22). The extra nucleotide alters and extends the translation of the *STE23* open reading such that amino acids 971-988 now code for 18 distinct amino acid and an additional 39 amino acids are gained as an extension to the original proposed translation.

***Protein Extract Preparations*** **-** Whole cell protein extracts for Western analysis were prepared by the NaOH/TCA method (23). In brief, mid-log cells (an amount equivalent to 2 ml of a 1.0 $OD_{600}$ culture) were harvested by centrifugation, washed once with cold water, resuspended in 1 ml of cold water, and treated with a solution of 2 N NaOH / 1 M βME. Proteins released were precipitated with TCA (11.5% final), recovered by centrifugation, resuspended in Urea Sample Buffer (USB; 250 mM Tris, pH 8.0, 6 M urea, 4% SDS, and 0.01% bromophenol blue), heated, and cleared of insoluble material before analysis by SDS-PAGE and immunoblotting. HA-tagged proteins were detected by chemilumenescence (ECL kit, Roche) after immundecorating proteins with mouse anti-HA and HRP-conjugated rabbit anti-mouse antibodies.

Particulate fractions used for *in vitro* assays were prepared by mechanical breakage of yeast cells expressing either IDE, Ste23p, or Axl1p (24,25). In brief, mid-log cells were harvested, washed with cold 10 mM $NaN_3$, and treated with Tris/DTT (100 mM Tris, pH 9.4, 10 mM DTT) for 10 min on ice. Cells were resuspended in Oxalyticase Buffer (50 mM KPi, pH 7.5, 1.4 M sorbitol, and 10 mM $NaN_3$) containing Oxalyticase (1 μg/$OD_{600}$; Enzogenetics, Corvallis, OR) and incubated for 30 min at 30 °C with gentle mixing. The spheroplasts were harvested by centrifugation, resuspended in cold Lysis Buffer (50 mM Tris, pH 7.5, 0.2 M sorbitol, and 1 mM

EDTA) containing protease inhibitors (1 μg/ml each leupeptin, chymostatin, pepstatin, aprotinin, and 1 mM PMSF), and lysed using a glass Dounce homogenizer. The primary lysate was cleared twice of cell debris by centrifugation (500 g, 10 min), and fractionated into supernatant and particulate fractions by centrifugation (16,000 g, 10 min). The fractions were adjusted to 1 mg/ml with Lysis buffer and stored at –80 °C as aliquots.

To assess the effect of chaotropic agents on the association of IDE, Ste23p, and Axl1p with the yeast particulate fraction, freshly prepared samples of the particulate fraction were exposed to either 1 M NaCl, 0.1 M $Na_2CO_3$ (pH 11.5), 1% SDS, or buffer alone for 10 min on ice, and the samples subjected to centrifugation (16,000 g, 10 min). Equivalent portions of each supernatant and particulate fraction were analyzed by SDS-PAGE and immunoblot as described above.

***Insulin Degradation Assay*** **-** Insulin degradation assays were carried out essentially as previously described, but using yeast-derived lysates as the source of enzyme activity (4). In brief, reactions were assembled to contain 0.5 mg/ml of yeast lysate and 60 pM (~10,000 cpm) of $^{125}$I-insulin (Linco Research, St. Charles, MO) in 50 μl of reaction buffer (50 mM Tris, 0.2 M sorbitol, pH 7.5, 1 mM EDTA). Samples were incubated at 37 °C for the times indicated in the appropriate figure legend. Final sample preparation involved the addition of BSA (1 % final), TCA precipitation (10 % final) for 10 min on ice, and centrifugation (16,000 g, 10 min) at 4°C. The supernatant containing insulin fragments was transferred to a new tube, and the radioactivity associated with the supernatant and particulate fractions was determined using a Wallac γ-counter (Perkin Elmer, Boston, MA).

***Yeast Mating Assay*** **-** To evaluate the ability of plasmid-transformed *MAT***a** *axl1*Δ *ste23*Δ strains to promote **a**-factor production, patch mating tests were performed using IH1793 (*MAT*α *lys1*)

and established methods (26). This test provides an indirect assessment of M16A enzyme function since **a**-factor production in the *MAT***a** cells is entirely dependent on the plasmid-encoded copy the M16A enzyme. In brief, master plates were prepared by patching *MAT***a** yeast strains expressing Axl1p, Ste23p, or IDE onto YEPD agar plates. After 2-3 days growth, the patches were replica printed onto lawns of *MAT*α cells (IH1793) and the replica printed plates incubated for 2 days at 30 °C. The *MAT*α cell suspensions were prepared to approximately the same cell density in solutions of 1, 10, or 100% YEPD, which were prepared as mixtures of YEPD and the appropriate amount of sterile $H_2O$. The trace amount of YEPD added to the minimal media allows for limited survival of the auxotrophic haploid cells, which is necessary for the mating process. Decreasing the YEPD amount shortens the survival window of the haploid cells and thus results in decreased mating efficiency. The diploid cells that result from mating events are prototrophic, and thus the growth of diploids in this test is indicative of mating and a functional M16A enzyme.

***Mass Spectroscopy* -** The **a**-factor mating pheromone produced by yeast expressing IDE, Ste23p, or Axl1p was purified according to published methods and analyzed by mass spectroscopy (26). In brief, yeast were cultured in polypropylene culture tubes, and **a**-factor secreted from the yeast cultures was recovered by washing the polypropylene culture tubes with methanol; secreted **a**-factor adsorbs to polypropylene and can be removed with organic solvents. The enriched **a**-factor samples were concentrated by speed-vac, desalted using Zip-tip C18 beads (Millipore), washed 3X with 0.1% trifluoroacetic acid, eluted with 70% acetonitrile, and subjected to MALDI-TOF/TOF mass spectroscopy using α-cyano-4-hydroxycinnamic acid matrix and a 4700 Proteomics Analyzer spectrometer (Applied Biosystems, Foster City, CA).

***a-factor Halo Assay -*** The total secreted **a**-factor produced by the saturated cultures of indicated strains was recovered as described above. The enriched samples were dried by speed-vac and resuspended in 50 µl of MeOH. Two-fold serial dilutions of the samples prepared in YEPD were spotted onto a lawn of RC757 (*MAT*α *sst2-1 his6 met1 can1 cyh2*) or RC631 (*MAT***a** *sst2-1 his6 met1 can1 cyh2 rme ade2-1 ura1*) cells; the latter served as a control for the unlikely possibility that a toxic product was being produced by the IDE-expressing strain (27). The formation of a spot in the lawn is indicative of the presence of pheromone in the sample, and the relative potency of pheromone can be determined from the serial dilutions of the sample. The highest dilution having biological activity is referred to the endpoint and is equivalent to a concentration of 12 pg/µl of **a**-factor (28).

***Invasive Growth Assay -*** The ability of haploid yeast cells to invade yeast agar was determined using a plate-washing assay (14). In brief, cell suspensions were spotted onto SC-ura plates and the cells were grown for 4 days at 30 °C. The plates were washed under running $H_2O$ while gently rubbing the surface of the agar plate with a gloved finger. Agar plates were scanned prior to and immediately after washing.

***Budding Assay -*** Mid-log cells grown in selective liquid media were harvested to concentrate the cell suspension ~2X, and the cells were treated with 10 µg/ml Calcofluor (Sigma-Aldrich) for 5 min. The cells were washed 2X with $H_2O$, absorbed onto polylysine coated glass slides, and viewed at 100X with a Zeiss Axioplan microscope equipped with fluorescence optics. Fluorescent images were captured using a digital camera (Optronics, DEI-750). Bud scars on 100 cells were evaluated and categorized into three patterns: axial, bipolar, and random. The

axial pattern was defined as bud scars located solely at one pole of the cell, the bipolar pattern had scars at both poles, and the random pattern displayed at least one bud scar in the region between both poles (8,9).

## RESULTS

***IDE can be heterologously expressed in yeast.*** Many of the yeast enzymes required for **a**-factor production can be functionally replaced with orthologs from other eukaryotic species (29-34). Thus, we hypothesized that IDE could rescue the mating defect of a strain lacking Axl1p and Ste23p. Prior to evaluating the ability of IDE to substitute for the functions of the yeast M16A enzymes, we first determined whether yeast could be used for the heterologous expression of IDE. We created plasmids encoding epitope-tagged versions of the genes encoding IDE and its yeast orthologs. For all the proteases, a DNA fragment encoding the HA epitope tag was placed at the 3' end of each gene. The addition of this tag did not alter the activities of these enzymes (see Fig. 2.3B).

Evaluation of protein extracts from strains expressing the tagged proteases revealed that each tagged protein could be detected as a protein of the expected size by immunoblot (Fig. 2.1A). We also observed that IDE and Ste23p were expressed at approximately 10X higher levels than Axl1p as determined by comparison of immunoblot signals. The constitutive phosphoglycerate kinase (*PGK*) promoter was used to drive IDE expression, so the abundant expression of IDE was not unexpected. Native promoters were used to drive Ste23p and Axl1p expression, and the relative abundance of Ste23p over Axl1p was somewhat unexpected, especially since Ste23p does not promote **a**-factor production as efficiently as Axl1p. Thus, the reason for the decreased ability of Ste23p to promote mating cannot be simply attributed to reduced protein expression by comparison to Axl1p.

***IDE is associated with a particulate yeast fraction.*** The subcellular distribution of IDE in mammalian systems is reported to be primarily cytosolic, with extracellular and peroxisomal localizations also being described (35,36). To ascertain the effect of heterologous expression on the subcellular distribution of IDE, we subjected a total yeast lysate to differential fractionation. By comparison of equal amounts of loaded protein by immunoblot, we observed that IDE and the yeast M16A enzymes were highly enriched in the particulate fraction associated with 16,000 x g centrifugation of the lysate (P16), although a significant amount of Ste23p was found in the supernatant fraction (Fig. 2.1B). In this particular experiment, Axl1p was encoded on a multi-copy plasmid to facilitate its detection, hence its stronger signal relative to that observed in total extracts (see Fig. 2.1A).

While the localization of Ste23p has not been previously reported, Axl1p is known to transiently associate with components that form a sub–plasma membrane complex that is required for establishing bud sites. Whether IDE or Ste23p can assemble into this complex is unknown. To better understand the nature of association that IDE, Axl1p, and Ste23p have with the P16 yeast fraction, we performed extractions of the particulate fraction with various chaotropic agents (Fig. 2.1C). Our analysis revealed that high pH and detergent treatments significantly disrupted the association of these proteins with the P16 fraction, whereas salt and buffer alone had a minor impact. This profile is consistent with IDE, Ste23p, and Ax1p being peripheral membrane proteins and/or components of a large macromolecular complex that sediments under our experimental conditions.

***Yeast-expressed IDE retains proteolytic activity.*** We next determined whether yeast-expressed IDE could cleave insulin, a well-characterized substrate of IDE, using a previously described insulin-degradation assay and yeast-derived particulate fractions (4,25). Because of

the high degree of enrichment for M16A enzymes in yeast particulate fractions, these samples were used exclusively as the source of activity for these *in vitro* assays. Our analysis of enzymatic activity indicated that the IDE-containing samples had insulin cleaving activity, whereas samples containing Axl1p or Ste23p had no more activity than a sample prepared from yeast lacking these enzymes (Fig. 2.2A). The source of the residual activity in these preparations is unknown, but is likely due to a non-specific enzymatic activity rather than that of an additional IDE homolog because 1,10-phenanthroline, a well-documented IDE inhibitor, does not inhibit the residual activity (Fig. 2.2B). Whether the Axl1p and Ste23p proteases in these preparations are incapable of cleaving insulin because of altered substrate specificity, sub-optimal reaction conditions, or other reasons has not yet been determined.

IDE is described as a thiol- and zinc-dependent metalloprotease (35). Having determined that IDE can be heterologously expressed in a functional form, we next wanted to confirm that the observed insulin degrading activity detected had the hallmarks of IDE-mediated insulin degradation. We examined the effect of alkylating (*e.g.*, iodoacetamide and NEM) and metal ion chelating agents (*i.e.*, 1,10-phenanthroline and EDTA) on IDE activity (Fig. 2.2B). Alkylating agents inhibited IDE-dependent insulin-degrading activity. An inhibitory effect was also observed for 1,10-phenanthroline, but not with the non-chelating agent 4,7-phenanthroline that is structurally similar. EDTA did not measurably inhibit enzymatic activity; extensive pre-treatment with EDTA is reportedly required for inhibition of IDE (15). The inhibitor profile observed for insulin-degrading activity in yeast was identical to that reported for IDE, which further establishes that yeast can synthesize IDE possessing all the enzymatic properties described for that of IDE found in metazoans (35).

***IDE can promote yeast mating.*** Many of the yeast enzymes required for **a**-factor production can be functionally replaced by orthologous enzymes from other species (29-34). In similar fashion, we have now determined that IDE expression can rescue the mating defect of a yeast strain lacking both *AXL1* and *STE23* (*MAT***a** *axl1*Δ *ste23*Δ) (Fig. 2.3A; top row). The mating defect in this strain is due to an inability to produce yeast **a**-factor, but whether Axl1p and Ste23p, and by extension IDE, participate directly or indirectly in pheromone production has not been rigorously established (9). Nevertheless, this result establishes that IDE and the yeast enzymes Axl1p and Ste23p can similarly promote yeast **a**-factor production and thus have an evolutionarily conserved activity. The simplest explanation for our findings is that these enzymes directly participate in pheromone production and that these enzymes have shared substrate specificity with respect to cleavage of the **a**-factor precursor.

Yeast mating is sensitive to a number of variables, including available nutrients. Under depleted nutrient conditions, mating is less efficient. We have taken advantage of this property of yeast mating to evaluate the effectiveness of IDE in rescuing the mating defect of yeast lacking both Ste23p and Axl1p. As expected, we observed that decreasing nutrient conditions correlated with decreased mating for all strains. Ste23p and IDE-expressing strains showed significant reductions in mating relative to the Axl1p expressing strain (Fig. 2.3A). Epitope tagged versions of these enzymes had a similar activity profile in this assay (Fig. 2.3B). The relatively poor ability of Ste23p to promote mating, with respect to Axl1p, is consistent with previous reports on the properties of this enzyme and may be attributable to a number of factors, including altered substrate specificity and/or an altered subcellular localization pattern that prevents interaction with substrates (9). Likewise, the reduced mating observed for IDE may be attributable to similar factors. The reduced mating observed for IDE and Ste23p-expressing cells

is not simply due to low expression of these enzymes since both are expressed at significantly higher levels than Axl1p (see Fig. 2.1).

The most straightforward explanation for the reduced mating observed with Ste23p and IDE-expressing strains is that these strains have reduced **a**-factor production by comparison to Axl1p-expressing strains. Thus, we compared the relative amounts of **a**-factor produced by these strains over the lifetime of a culture. We used a bioassay that relies on the natural growth-arrest response of *MAT*α cells to the **a**-factor pheromone to detect and quantifiably measure **a**-factor activity in our samples. Our analysis revealed that both IDE and Ste23p expressing strains produce significantly less **a**-factor than an Axl1p expressing strain despite the fact that IDE and Ste23p are significantly over-expressed relative to Axl1p (Fig. 2.3C). The IDE-derived sample was also bioassayed using *MAT***a** cells. These cells fail to undergo growth arrest in response to the **a**-factor pheromone, and thus served as a control for the unlikely scenario that IDE-expressing strains were producing a toxic secreted product. No growth inhibition of *MAT***a** cells was observed with the IDE-derived sample (Fig. 2.3D).

The **a**-factor mating pheromone is an isoprenylated and carboxylmethlated dodecapeptide (YIIKGVFWDPAC[farnesyl]-methyl). Alternations to the chemical form of **a**-factor (*e.g.*, lipid removal or primary sequence alterations) can impact the function of this pheromone (37). For example, **a**-factor lacking a tyrosine residue has 25% of the biological activity of full-length pheromone as judged by yeast mating tests (37). Thus, the reduced production of **a**-factor pheromone by IDE and Ste23p-expressing yeast could be attributable to cleavage of the **a**-factor precursor at a site other than the Asn-Tyr cleavage site recognized by Axl1p. To determine whether the pheromone products produced by IDE, Ste23p, and Axl1p were identical, we determined the mass of the **a**-factor species generated by these enzymes using MALDI-

TOF/TOF mass spectroscopy. Several major species were detected in these samples, including a 1629 Da peak that corresponds exactly to the mass of *bona fide* **a**-factor (Figs. 2.4A-C; IDE, Ste23p, and Axl1p samples, respectively). This species was not in the negative control (Fig. 2.4D). The 1629 Da species was still observed in the samples after the data was deisotoped (Fig 2.4E-G), and remained absent in the negative control (Fig. 2.4H). Based on these observations, we reason that the 1629 Da species is indeed **a**-factor, which implies that IDE, Ste23p and Axl1p have similar cleavage specificities.

Although no other species were apparent in the deisotoped data for the IDE and Ste23p-derived samples in the indicated mass range, additional species were evident in the other samples. In the Axl1p-derived sample, three additional species were observed (1480, 1526, and 1718 Da) (Fig. 2.4G). One distinct species was observed in the negative control (1587 Da). These additional species were not reproducibly detected between experiments[3]. The mass range shown in all panels is inclusive of the masses of theoretical *MFA1*-derived **a**-factor species either lacking an N-terminal tyrosine (1467 Da) or extended by an N-terminal asparagine (1744 Da), but none of the four unidentified species can be matched to these alternative **a**-factor cleavage products. The nature of these other species is therefore unknown.

The ability of yeast-expressed IDE to promote **a**-factor production suggests that yeast mating can be used as a phenotype to evaluate the function of IDE mutant alleles. To test this hypothesis, we created site-directed and deletion mutations of IDE and tested the ability of these mutants to promote mating. Using our genetic system, we confirmed that residues comprising the core metalloprotease motif (*HxxEH*) of IDE were essential for promoting mating (Fig. 2.5A). These residues were required for the activity of Ste23p and Axl1p as well (Figs. 2.5B and

[3] unpublished observation

5C, respectively). The most distal glutamate of the extended motif (*HxxEHx$_{69}$Ex$_{69}$E*) was also determined to be essential for the activity of all three enzymes, whereas the penultimate glutamate was dispensable for Axl1p activity. The penultimate glutamate is also required for the activity of Mitochondrial Processing Peptidase (MPP), an M16B protease, and has been proposed to aid in metal coordination of this enzyme (38).

In addition to addressing the importance of established active site residues, we investigated the functional importance of cysteine residues in the function of IDE. We initially investigated the role of two cysteine residues that are invariably conserved between IDE, Ste23p, and Axl1p (*HxCEHx$_{69}$Ex$_{6}$Ex$_{67}$C*), suspecting that one of these residues is the likely target of sulfhydryl modifying agents that inactivate certain M16A enzymes. Independent mutations at these residues did not alter the abilities of IDE, Ste23p, or Axl1p to promote mating (Fig. 2.5). Mutation of the proximal cysteine of IDE ($C_{110}A$) reportedly does not alter the thiol-sensitivity profile of IDE (15), and similarly, we found that mutation of the distal cysteine of IDE ($C_{257}A$) had no effect on the thiol sensitivity of IDE[4]. We also determined that combining the mutations in one molecule ($C_{110}A/C_{257}A$) did not alter mating function (Fig. 2.5A). Moreover, the sensitivity of IDE to thiol modifiers was unaffected[5]. Similar results were observed when other cysteine residues that are conserved between IDE and Ste23p or Axl1p ($C_{819}A$ and $C_{414}A$, respectively) were mutated (Fig. 2.5A).

M16A enzymes are large proteins, typically having a molecular mass in excess of 100,000 Da. The metalloprotease motif of M16A enzymes is localized near the N-terminal end of these enzymes. In the absence of structural data for these enzymes, we sought to determine whether the catalytic domain of IDE was self-contained within the N-terminal portion of the enzyme. C-

[4] unpublished observation
[5] unpublished observation

terminally truncated forms of IDE were created and evaluated for the ability to promote pheromone production. These truncations were created as fusions to GFP, which in and of itself did not alter the ability of IDE to function (Fig 2.6A; IDE 1-1019). Systematic deletions of the C-terminus of IDE revealed that relatively short truncations inactivated IDE as judged by yeast mating tests. Deletion analysis of Axl1p revealed a similar requirement for an intact C-terminus, although the deletion required for Axl1p inactivation was considerably larger (Fig. 2.6A; Axl1p 1-1076). Site-directed mutation of a residue conserved between IDE and Axl1p that was at the functional/non-functional truncation boundary of Axl1p (*i.e.*, $Ser_{965}$ in IDE and $Ser_{1081}$ in Axl1p) did not reveal an essential requirement for this residue in either enzyme (Fig. 2.5).

For the site-directed and truncation mutants created for this study, we evaluated protein expression. Using immunoblots, the site-directed mutants were judged to be expressed as well as the relevant wildtype control, except for Ste23p $E_{192}A$ that was expressed at a level approximately one quarter that of wildtype[6]. With the exception of this mutant, our results rule out the trivial possibility that inactive IDE, Axl1p, and Ste23p mutants are nonfunctional due to poor expression. We cannot exclude the possibility that these mutants are non-functional due to malfolding or other unknown reasons. Evaluation of the Axl1p truncation mutants revealed that these were expressed at levels similar to that of the full-length Axl1p-GFP fusion protein. By contrast, the IDE truncation mutants were not similarly expressed (Fig. 2.6B). We observed decreased expression for certain truncations, suggesting that the C-terminus of IDE, for reasons unknown, is required for normal steady state expression. Decreased expression alone cannot account for the loss of activity for IDE, since one non-functional truncation (IDE 1-973) was expressed comparably to the full length IDE-GFP fusion. Importantly, the expression levels

[6] unpublished observation

observed for all the non-functional truncations of Axl1p and IDE, which were encoded on multi-copy plasmids, were significantly more than that of the respective full-length fusion encoded on a low-copy plasmid, as judged by immunoblot analysis, suggesting that lowered expression alone cannot account for the absence of function in these mutants.

***Yeast-expressed IDE cannot substitute for other known functions of Axl1p.*** Axl1p is involved in regulating several cellular processes besides pheromone production. For example, Axl1p is required for repressing haploid invasive growth (14). Haploid invasion occurs more readily upon the deletion of *AXL1*, and this phenotype can be fully reversed by the introduction of a plasmid-born copy of *AXL1*. In order to address the ability of IDE to substitute for this other function of Axl1p, the invasive phenotype of an Axl1p-deficient strain (*axl1*) that expressed IDE was examined. We also investigated the ability of a protease active site mutant of Axl1p to suppress invasive growth. We found that IDE-expression could not repress invasive growth, whereas the Axl1p active site mutant suppressed invasive growth (Fig. 2.7).

Axl1p also has a well-described role in the maintenance of the axial budding pattern of haploid yeast (9). Ste23p does not reportedly have a role in this process. To determine whether IDE could substitute for the function of Axl1p in axial bud site selection, we expressed IDE in a haploid strain defective for axial budding and evaluated the budding pattern by Calcofluor staining of bud scars. Consistent with previous findings, we observed a bipolar budding phenotype in the absence of Axl1p expression (Table 2.3; vector). An axial budding phenotype was observed upon the introduction of a plasmid encoding Axl1p into the *axl1* strain (*AXL1*), whereas bipolar budding was the predominant pattern when either *STE23* or IDE was introduced.

## DISCUSSION

The majority of studies on the insulin-degrading enzyme (IDE) have relied on *in vitro* biochemical assays (1). More recently, knock-out and over-expression mouse models have been described for IDE (4-6). Both *in vitro* and *in vivo* model systems have led to a better understanding of the biochemical and physiological properties of IDE, which has proposed roles in type 2 diabetes and Alzheimer disease (4,39-41).

In this study, we have developed yeast as a tractable genetic model system for studying the functional properties of IDE. We have determined that yeast can be used to express a functional form of IDE, and importantly, that IDE can promote **a**-factor production, an activity normally associated with the yeast enzymes Axl1p and Ste23p that have homology to IDE. These results imply that members of the M16A metalloprotease family, to which these enzymes belong, may have shared substrate specificity. The fact that all three enzymes can promote **a**-factor production supports this hypothesis. However, our inability to demonstrate insulin cleavage by the yeast enzymes implies that the substrate specificity of Ste23p and Axl1p may be more restricted. Whether the yeast enzymes cleave other established IDE substrates is currently under investigation. We are also investigating the ability of other M16A enzymes to cleave **a**-factor, since the studies of these enzymes may benefit from the development of a tractable genetic system.

An additional finding from our study is that IDE is enriched but does not exclusively partition into a yeast particulate fraction. We suspect that heterologously expressed IDE is either being incorporated into membranes as a loosely associated peripheral membrane protein or it is assembling into a macromolecular complex that partially sediments under the conditions used for isolation of the particulate fraction. While IDE reportedly associates with peroxisomes, this

localization is unlikely under our experimental conditions since we did not impose an induction that is required for the formation of yeast peroxisomes (42). Moreover, the putative C-terminal peroxisomal targeting signal found in IDE, while potentially functional in yeast, is blocked by an epitope tag in our yeast expressed enzyme. Alternatively, IDE may be associating with other undefined membrane sites. Axl1p has been reported to transiently associate with components that form a sub-plasma membrane complex that is required for budding (43). Thus, it is also conceivable that IDE is assembling into this complex, but as a non-functional component. Ultimately, defining the subcellular localization Ste23p may provide insight into the subcellular targeting of IDE since these two enzymes appear more conserved in sequence and enzymatic properties than IDE and Axl1p.

The genetic model system that we have developed should have far reaching utility for the characterization of mutant IDE alleles. We have provided a practical example of this utility by detailing the functional importance of residues that comprise the extended metalloprotease motif (*HxxEHx$_{69}$Ex$_6$E*). In addition, our mutational study allows us to make certain conclusions about the cysteine residue(s) that imparts the sensitivity of IDE to thiol modifiers. Provided that a single cysteine residue is the target of thiol modification in IDE, our study excludes as targets the two cysteine residues that are invariably conserved between all three enzymes ($C_{110}$ and $C_{257}$ in IDE) and two cysteines that are semi-conserved between IDE and the yeast M16A enzymes ($C_{414}$ and $C_{819}$ in IDE). The double $C_{110}A/C_{257}A$ mutant also remains sensitive to thiol modifiers. We are currently developing an *in vitro* assay for monitoring the activities of Ste23p and Axl1p. We expect a determination of whether these enzymes are sensitive to thiol-modifiers to aid in the final identification of cysteine residues that are targeted by thiol-modifiers in this enzyme family. As a second practical example of the utility of our genetic system, we demonstrate for the first

time that a C-terminal region is required for the activity of IDE. In the absence of structural information for IDE, we suspect that its C-terminal region may be required for stabilizing the overall tertiary or possibly quaternary structure of IDE or its active site.

Our genetic system will also be useful for investigating the role of other residues in the function of IDE. For example, several conserved sequence motifs can be identified by multiple-sequence alignment of M16A enzymes (Fig. 2.8). Our future studies will be aimed at determining whether these motifs are important for the function of M16A enzymes. In addition, we will investigate whether *E. coli* Protease III can support **a**-factor production in yeast. If so, our system could conceivably be used to investigate the structure function relationships for this enigmatic protease, which also lacks a defined cellular role (44).

Another potential utility of our genetic model system is the theoretical ability to rapidly identify IDE mutants having altered substrate specificity. We have already demonstrated that our system is amenable to screening specific mutant IDE alleles for the ability to promote mating. The same approach could be used to identify IDE mutants having altered specificity toward **a**-factor. We envision a positive genetic selection that takes advantage of the observations that IDE-dependent mating is essentially non-existent at reduced nutrient levels (Fig. 2.3A). Under these highly stringent mating conditions, yeast harboring IDE mutants could be screened with the expectation that those having enhanced **a**-factor production would now be mating competent. These IDE mutants would represent candidates having improved **a**-factor recognition (*i.e.*, altered substrate specificity). Conceivably, these mutants might also have altered specificity for insulin and/or Aβ. IDE mutants having enhanced activity toward these substrates could potentially be used as therapeutic agents for diabetes or Alzheimer disease.

Our data clearly demonstrates that the Axl1p/Ste23p-dependent step in **a**-factor production can be supported by IDE. This result, in and of itself, is not surprising given the high degree of similarity between these enzymes. Of greater curiosity is the observation that all the yeast enzymes required for **a**-factor production can be functionally replaced by their mammalian counterparts. The first three steps associated with **a**-factor production (*i.e.*, isoprenylation, *CaaX* proteolysis, and carboxylmethylation) are part of the biosynthetic pathway of isoprenylated proteins, such as Ras and RhoB. The subsequent two proteolytic steps associated with **a**-factor production have no analogous counterparts in mammals. Thus, the ability of mammalian enzymes to promote these latter steps is entirely serendipitous, or it reflects the existence of an orphan biosynthetic pathway that integrates all the steps associated with **a**-factor biosynthesis. If the latter, by analogy, we suspect that the molecule produced by this pathway would serve as a secreted signaling molecule, possibly functioning to regulate cell-cell fusion events such as those that occur during the development of certain tissues. Curiously, the morphological and biochemical differentiation of $L_6$ myoblasts into myotubes has been reported to involve IDE (45,46). Thus, by analogy to **a**-factor production, we hypothesize that a role of IDE in these cells might be to produce a signaling molecule derived from a precursor having a *CaaX* motif and an N-terminal extension that is readily cleaved by IDE. Whether such a molecule exists in mammalian systems remains to be determined.

## ACKNOWLEDGMENTS

We are grateful to Drs. Claiborne Glover, Michelle Momany, Ron Orlando, Lance Wells, and members of their respective laboratories for technical advice, access to equipment, and critical discussions. This work was supported by funds from the University of Georgia. SK is supported through a UGA Graduate School Assistantship.

**REFERENCES**


1. Becker, A. B., and Roth, R. A. (1995) *Methods Enzymol* **248**, 693-703
2. Qiu, W. Q., Walsh, D. M., Ye, Z., Vekrellis, K., Zhang, J., Podlisny, M. B., Rosner, M. R., Safavi, A., Hersh, L. B., and Selkoe, D. J. (1998) *J Biol Chem* **273**, 32730-32738
3. Edbauer, D., Willem, M., Lammich, S., Steiner, H., and Haass, C. (2002) *J Biol Chem* **277**, 13389-13393
4. Farris, W., Mansourian, S., Chang, Y., Lindsley, L., Eckman, E. A., Frosch, M. P., Eckman, C. B., Tanzi, R. E., Selkoe, D. J., and Guenette, S. (2003) *Proc Natl Acad Sci U S A* **100**, 4162-4167
5. Leissring, M. A., Farris, W., Chang, A. Y., Walsh, D. M., Wu, X., Sun, X., Frosch, M. P., and Selkoe, D. J. (2003) *Neuron* **40**, 1087-1093
6. Miller, B. C., Eckman, E. A., Sambamurti, K., Dobbs, N., Chow, K. M., Eckman, C. B., Hersh, L. B., and Thiele, D. L. (2003) *Proc Natl Acad Sci U S A* **100**, 6221-6226
7. Tanzi RE, M. R., Wagner SL. (2004) *Neuron* **43**, 605-608
8. Fujita, A., Oka, C., Arikawa, Y., Katagai, T., Tonouchi, A., Kuhara, S., and Misumi, Y. (1994) *Nature* **372**, 567-570
9. Adames, N., Blundell, K., Ashby, M. N., and Boone, C. (1995) *Science* **270**, 464-467
10. Chen, P., Sapperstein, S., Choi, J. D., and Michaelis, S. (1997) *J. Cell. Biol.* **136**, 251-269
11. Elia, L., and Marsh, L. (1998) *J Cell Biol* **142**, 1473-1485
12. Brizzio, V., Gammie, E., Nijbroek, G. L., Michaelis, S., and Rose, M. (1996) *J. Cell Biol.* **135**
13. Palecek, S. P., Parikh, A. S., and Kron, S. J. (2000) *Genetics* **156**, 1005-1023

14. Cullen, P. J., and Sprague, G. F., Jr. (2002) *Mol Biol Cell* **13**, 2990-3004

15. Perlman, R. K., Gehm, B. D., Kuo, W. L., and Rosner, M. R. (1993) *J Biol Chem* **268**, 21538-21544

16. Perlman, R. K., and Rosner, M. R. (1994) *J. Biol. Chem.* **269**, 33140-33145

17. Ding, L., Becker, A. B., Suzuki, A., and Roth, R. A. (1992) *J Biol Chem* **267**, 2414-2420

18. Elble, R. (1992) *BioTechniques* **13**, 18-20

19. Michaelis, S., and Herskowitz, I. (1988) *Mol. Cell. Biol.* **8**, 1309-1318

20. Oldenburg, K. R., Vo, K. T., Michaelis, S., and Paddon, C. (1997) *Nucleic Acids Res* **25**, 451-452

21. Seta, K. A., and Roth, R. A. (1997) *Biochem Biophys Res Commun* **231**, 167-171

22. Brachat, S., Dietrich, F. S., Voegeli, S., Zhang, Z., Stuart, L., Lerch, A., Gates, K., Gaffney, T., and Philippsen, P. (2003) *Genome Biol* **4**, R45

23. Fujimura-Kamada, K., Nouvet, F. J., and Michaelis, S. (1997) *J. Cell Biol.* **136**, 271-285

24. Schmidt, W. K., Tam, A., Fujimura-Kamada, K., and Michaelis, S. (1998) *Proc Natl Acad Sci USA* **95**, 11175-11180

25. Schmidt, W. K., Tam, A., and Michaelis, S. (2000) *J. Biol. Chem.* **275**, 6227-6233

26. Nijbroek, G. L., and Michaelis, S. (1998) *Methods Enzymol* **292**, 193-212

27. Chan, R. K., and Otte, C. A. (1982) *Mol. Cell. Biol.* **2**, 11-20

28. Marcus, S., Caldwell, G. A., Miller, D., Xue, C.-B., Naider, F., and Becker, J. M. (1991) *Mol. Cell. Biol.* **11**, 3603-3612

29. Yalovsky, S., Trueblood, C. E., Callan, K. L., Narita, J. O., Jenkins, S. M., Rine, J., and Gruissem, W. (1997) *Mol. Cell. Biol.* **17**, 1986-1994

30. Dai, Q., Choy, E., Chiu, V., Romano, J., Slivka, S. R., Steitz, S. A., Michaelis, S., and Philips, M. R. (1998) *J. Biol. Chem.* **273**, 15030-15034

31. Tam, A., Nouvet, F., Fujimura-Kamada, K., Slunt, H., Sisodia, S. S., and Michaelis, S. (1998) *J. Cell Biol.* **142**, 635-649

32. Bracha, K., Lavy, M., and Yalovsky, S. (2002) *J Biol Chem* **277**, 29856-29864

33. Cadiñanos, J., Schmidt, W. K., Fueyo, A., Varela, I., Lopez-Otin, C., and Freije, J. M. (2003) *Biochem J* **370**, 1047-1054

34. Cadiñanos, J., Varela, I., Mandel, D., Schmidt, W. K., Díaz-Perales, A., López-Otín, C., and JMP, F. (2003) *Journal of Biological Chemistry* **278**, 42091-42097

35. Duckworth, W. C., Bennett, R. G., and Hamel, F. G. (1998) *Endocr Rev* **19**, 608-624

36. Morita, M., Kurochkin, I. V., Motojima, K., Goto, S., Takano, T., Okamura, S., Sato, R., Yokota, S., and Imanaka, T. (2000) *Cell Struct Funct* **25**, 309-315

37. Caldwell, G. A., Wang, S.-H., Xue, C.-B., Jiang, Y., Lu, H.-F., Naider, F., and Becker, J. M. (1994) *J. Biol. Chem.* **269**, 19817-19826

38. Striebel, H. M., Rysavy, P., Adamec, J., Spizek, J., and Kalousek, F. (1996) *Arch Biochem Biophys* **335**, 211-218

39. Fakhrai-Rad, H., Nikoshkov, A., Kamel, A., Fernstrom, M., Zierath, J. R., Norgren, S., Luthman, H., and Galli, J. (2000) *Hum Mol Genet* **9**, 2149-2158

40. Karamohamed, S., Demissie, S., Volcjak, J., Liu, C., Heard-Costa, N., Liu, J., Shoemaker, C. M., Panhuysen, C. I., Meigs, J. B., Wilson, P., Atwood, L. D., Cupples, L. A., and Herbert, A. (2003) *Diabetes* **52**, 1562-1567

41. Farris, W., Mansourian, S., Leissring, M. A., Eckman, E. A., Bertram, L., Eckman, C. B., Tanzi, R. E., and Selkoe, D. J. (2004) *Am J Pathol* **164**, 1425-1434

42. Lazarow, P. B. (2003) *Curr Opin Cell Biol* **15**, 489-497

43. Lord, M., Inose, F., Hiroko, T., Hata, T., Fujita, A., and Chant, J. (2002) *Curr Biol* **12**, 1347-1352

44. Barrett, A. J., Rawlings, N.D., Woessner, J.F. (2004) *Handbook of Proteolytic Enzymes*, 2nd Ed., 1. 2 vols., Elsevier Academic Press

45. Kayalar, C., and Wong, W. T. (1989) *J Biol Chem* **264**, 8928-8934

46. Kayalar, C., Wong, W. T., and Hendrickson, L. (1990) *J Cell Biochem* **44**, 137-151

47. Sikorski, R. S., and Hieter, P. (1989) *Genetics* **122**, 19-27

**Table 2.1. Strains used in this study.**

| Strain | Genotype[a] | Reference |
|---|---|---|
| IH1783 | *MAT***a** *trp1 leu2 ura3 his4 can1* | (19) |
| IH1793 | *MAT*α *lys1* | (19) |
| RC631 | *MAT***a** *sst2-1 his6 met1 can1 cyh2 rme ade2-1 ura1* | (27) |
| RC757 | *MAT*α *sst2-1 his6 met1 can1 cyh2* | (27) |
| Sy3687 | *MAT*α *ura3 his3::ura3* | (14) |
| Sy3721 | *MAT*α *ura3 his3::ura3 axl1::HIS3* | (14) |
| Y272 | *MAT***a** *trp1 leu2 ura3 his4 can1 axl1::LEU2 ste23::LEU2* | (9) |
| YPH499 | *MAT***a** *ura3-52 lys2 ade2 trp1 his3 leu2* | (47) |

[a]IH1783, IH1793, and Y272 are isogenic, as are Sy3687 and Sy3721.

**Table 2.2. Plasmids used in this study.**

| Plasmid | Genotype | Reference |
|---|---|---|
| p80 | *CEN URA3 AXL1* | (9) |
| p137 | *CEN URA3 STE23* | (9) |
| pRS316 | *CEN URA3* | (47) |
| pSRα-rat IDE | *ratIDE* | (21) |
| pSM463 | *2μ TRP1 MFA1* | (10) |
| pSM703 | *2μ URA3* $P_{PGK}$ | (33) |
| pWS371 | *CEN URA3 AXL1-2HA* | This study |
| pWS372 | *2μ URA3 AXL1-2HA* | This study |
| pWS380 | *2μ URA3 AXL1[1-1208]-GFP* | This study |
| pWS388 | *CEN URA3 axl1-2HA* $H_{68}A$ | This study |
| pWS389 | *CEN URA3 axl1-2HA* $E_{71}A$ | This study |
| pWS390 | *CEN URA3 axl1-2HA* $H_{72}A$ | This study |
| pWS391 | *CEN URA3 AXL1-2HA* $E_{149}A$ | This study |
| pWS392 | *CEN URA3 axl1-2HA* $E_{156}A$ | This study |
| pWS482 | *CEN URA3 STE23-2HA* | This study |
| pWS491 | *2μ URA3* $P_{PGK}$*-IDE* | This study |
| pWS496 | *2μ URA3* $P_{PGK}$*-IDE-2HA* | This study |
| pWS511 | *2μ URA3* $P_{PGK}$*-IDE-HA* | This study |
| pWS512 | *CEN URA3 ste23-2HA* $E_{121}A$ | This study |
| pWS513 | *CEN URA3 ste23-2HA* $E_{199}A$ | This study |
| pWS514 | *CEN URA3 ste23-2HA* $H_{118}A$ | This study |
| pWS515 | *CEN URA3 ste23-2HA* $H_{122}A$ | This study |
| pWS527 | *CEN URA3 STE23-2HA* $C_{120}A$ | This study |
| pWS531 | *2μ URA3* $P_{PGK}$*-IDE-HA* $H_{108}A$ | This study |
| pWS532 | *2μ URA3* $P_{PGK}$ *IDE-HA* $C_{110}A$ | This study |
| pWS533 | *2μ URA3* $P_{PGK}$ *IDE-HA* $E_{111}A$ | This study |
| pWS534 | *CEN URA3 AXL1-2HA* $C_{70}A$ | This study |
| pWS538 | *2μ URA3* $P_{PGK}$ *IDE[1-1019]-GFP* | This study |
| pWS539 | *2μ URA3* $P_{PGK}$ *IDE[1-960]-GFP* | This study |
| pWS541 | *2μ URA3 AXL1[1-1081]-GFP* | This study |
| pWS548 | *2μ URA3* $P_{PGK}$ *IDE[1-965]-GFP* | This study |
| pWS549 | *2μ URA3* $P_{PGK}$ *IDE[1-968]-GFP* | This study |
| pWS550 | *2μ URA3* $P_{PGK}$ *IDE[1-973]-GFP* | This study |
| pWS551 | *2μ URA3 axl1[1-1076]-GFP* | This study |
| pWS552 | *2μ URA3 AXL1[1-1084]-GFP* | This study |
| pWS553 | *2μ URA3 AXL1[1-1089]-GFP* | This study |
| pWS567 | *CEN URA3 ste23-2HA* $E_{192}A$ | This study |
| pWS568 | *2μ URA3 AXL1-2HA* $S_{1081}A$ | This study |
| pWS569 | *CEN URA3 AXL1-2HA* $C_{224}A$ | This study |
| pWS571 | *CEN URA3 STE23-2HA* $C_{267}A$ | This study |
| pWS572 | *2μ URA3* $P_{PGK}$ *IDE-HA* $C_{257}A$ | This study |
| pWS573 | *2μ URA3* $P_{PGK}$ *IDE-HA* $S_{965}A$ | This study |
| pWS590 | *2μ URA3* $P_{PGK}$ *IDE-HA* $H_{112}A$ | This study |
| pWS591 | *2μ URA3* $P_{PGK}$*-IDE-HA* $E_{182}A$ | This study |

| | | |
|---|---|---|
| pWS592 | *2μ URA3* $P_{PGK}$ *IDE-HA* $E_{189}A$ | This study |
| pWS598 | *2μ URA3* $P_{PGK}$ *IDE-HA* $C_{414}A$ | This study |
| pWS599 | *2μ URA3* $P_{PGK}$ *IDE-HA* $C_{819}A$ | This study |
| pWS600 | *2μ URA3* $P_{PGK}$ *IDE-HA* $C_{110}A$, $C_{257}A$ | This study |

**Table 2.3. Budding patterns observed for Axl1p, Ste23p, and IDE expressing strains.**

| Plasmid[a] | Genotype | Axial[b] | Bipolar | Random |
|---|---|---|---|---|
| pRS316 | vector | 26 | 64 | 10 |
| pWS371 | *AXL1* | 95 | 2 | 3 |
| pWS482 | *STE23* | 19 | 49 | 32 |
| pWS511 | IDE | 26 | 58 | 16 |

[a]the indicated plasmid was transformed into Y272; [b]n = 100 cells for each condition.

**Fig. 2.1.** *Yeast-expressed IDE is of the expected size and is associated with a particulate fraction*.

A) Protein extracts were prepared from yeast containing an empty vector, or vectors encoding HA-tagged Axl1p, Ste23p, or IDE. Equivalent amounts of each sample (lanes 1-3 and 9) and two-fold serial dilutions of Ste23p (lanes 4-8) and IDE (lanes 10-14) samples were analyzed by SDS-PAGE and immunoblot using an anti-HA antibody. B) A total yeast lysate containing HA-tagged IDE was subjected to differential centrifugation at 16,000 g. Corresponding particulate (P) and supernatant (S) fractions were recovered and equivalent amounts of protein (10 μg) were analyzed by SDS-PAGE and immunoblotting with the HA monoclonal antibody. C) Samples of yeast particulate fractions containing epitope-tagged Axl1p, Ste23p or IDE (top to bottom, respectively) were treated with either Lysis Buffer, 1 M NaCl, 0.1 M $Na_2CO_3$ (pH 11.5), or 1% SDS then separated into supernatant (S) and particulate (P) fractions by centrifugation. An equivalent percentage of each sample was evaluated by SDS-PAGE and immunoblot using the anti-HA antibody. The strains used were Y272 transformed with pRS316 (vector), pWS482 (*STE23-2HA*), pWS496 (*IDE-2HA*), and either pWS371 (*AXL1-2HA*; panel A) or pWS372 (*AXL1-2HA*; panels B-C).

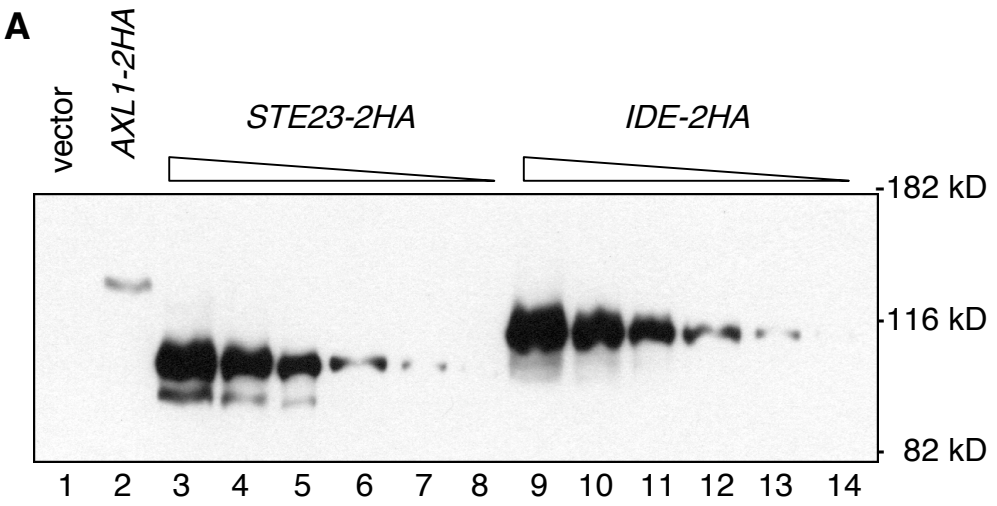
A
vector
AXL1-2HA
STE23-2HA
IDE-2HA
182 kD
116 kD
82 kD
1 2 3 4 5 6 7 8 9 10 11 12 13 14

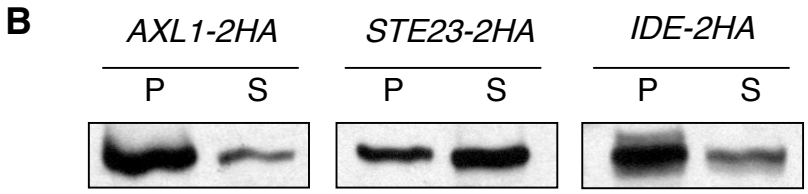
B
AXL1-2HA
STE23-2HA
IDE-2HA
P S P S P S

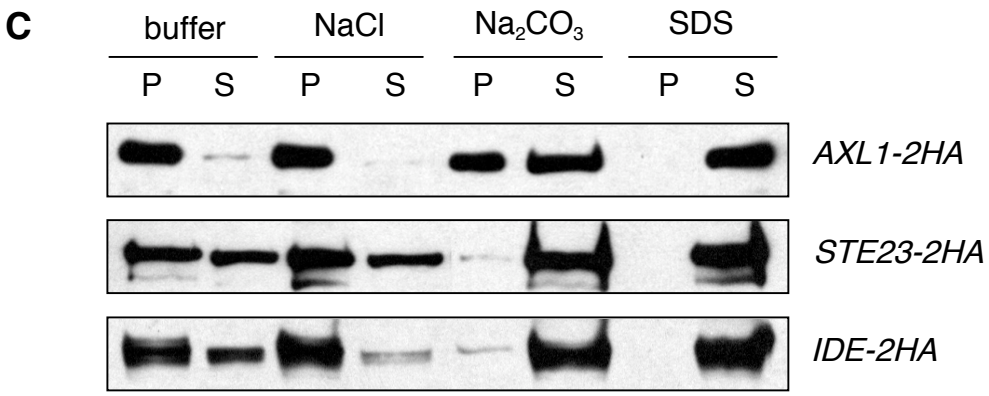
C
buffer
NaCl
Na2CO3
SDS
P S P S P S P S
AXL1-2HA
STE23-2HA
IDE-2HA

**Fig. 2.2.** *IDE can be functionally expressed in yeast*.

A) Particulate fractions were isolated from yeast expressing IDE, Axl1p, or Ste23p. An equivalent amount of each fraction (5 μg) was assayed for insulin degradation activity during a time course according to established methods (see Materials and Methods). The degradation of insulin is indicated by the presence of recovered insulin fragments that cannot be precipitated by TCA. B) The effect of various agents on the activity of yeast expressed IDE was evaluated. Activities were determined as in A, but only for the t = 0 min and t = 120 min time points. Abbreviations are NEM (1 mM N-ethylmalaemide), IAA (1 mM iodoacetamide), 1,10 (1 mM 1,10-phenanthroline), 4,7 (1 mM 4,7-phenanthroline), and EDTA (10 mM ethylenediaminetetraacetic acid).

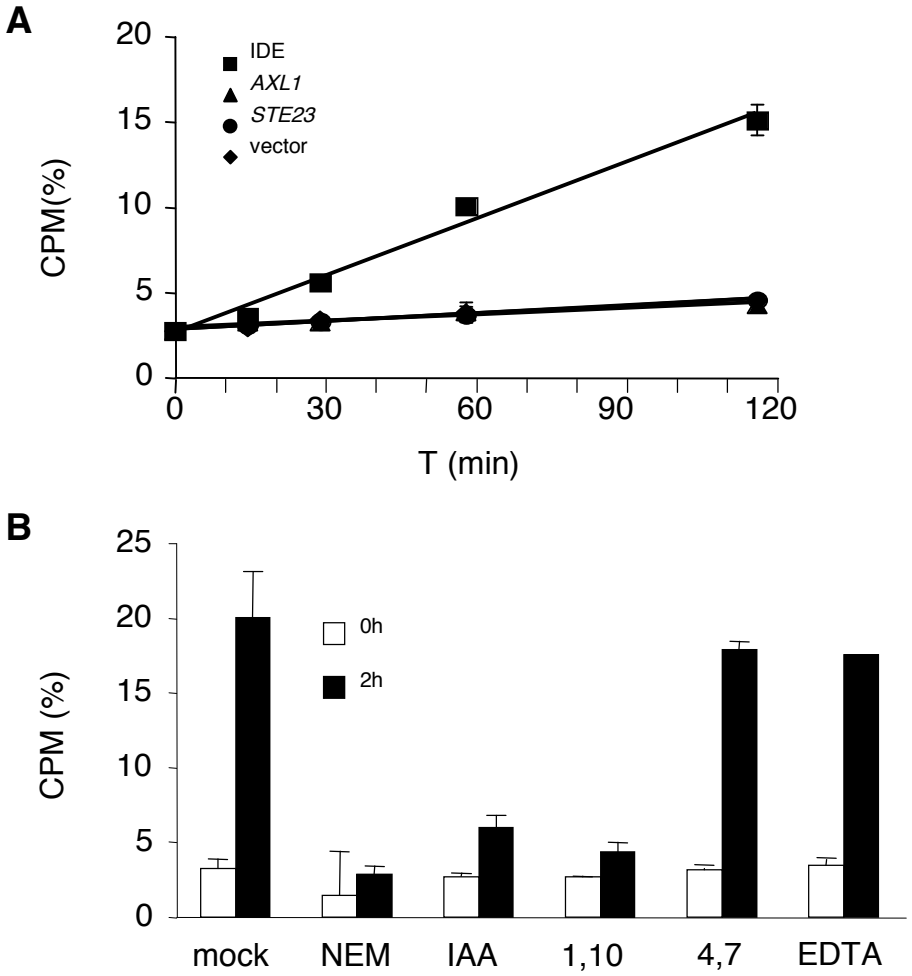
A
20
15
10
5
0
CPM(%)
IDE
AXL1
STE23
vector
0
30
60
90
120
T (min)
B
25
20
15
10
5
0
CPM (%)
0h
2h
mock
NEM
IAA
1,10
4,7
EDTA

**Fig. 2.3.** *Yeast-expressed IDE promotes yeast mating and* ***a****-factor pheromone production*.

A) The mating competence of *MAT***a** *ste23*Δ *axl1*Δ cells transformed with the indicated M16A enzyme encoded on a plasmid was evaluated using a patch mating test. The selective growth of diploid cells on the minimal media is indicative of mating. Patch mating tests were conducted using *MAT*α *lys1* lawns containing various amounts of nutrients (100%, 10% and 1% YEPD; top to bottom). Lowering the amount of YEPD in the lawn increases the stringency of the mating test and allows for discrimination of differences in mating efficiency not otherwise observable under permissive mating conditions (100% YEPD). B) Patch mating tests were conducted as in A but using *MAT***a** strains expressing HA-epitope tagged M16A proteases under mildly stringent mating conditions (10% YEPD). C) The **a**-factor produced by each of the strains described in B was recovered from the walls of culture tubes using an organic solvent, and concentrated samples were analyzed by a spot halo test. Each strain was grown to saturation in the same volume of media. The formation of a spot in the lawn of *MAT*α(RC757) cells is indicative of the presence of pheromone in the sample, and the relative pheromone potency can be determined by serial dilution of the sample. The highest dilution having activity is referred to the endpoint and is equivalent to a concentration of 12 pg/µl of **a**-factor (28). D) Two-fold serial dilutions of the IDE sample prepared in YEPD were spotted onto a lawn of RC631 (*MAT***a** *sst2-1 his6 met1 can1 cyh2 rme ade2-1 ura1*) serving as a control for the possibility that a toxic product was being produced by the IDE-expressing strain (27).The strains used were IH1783 transformed with pRS316 (WT), and Y272 transformed with pRS316 (vector), p80 (*AXL1*), p137 (*STE23*), pWS491 (*IDE*), pWS371 (*AXL1-2HA*), pWS482 (*STE23-2HA*), or pWS496 (*IDE-2HA*).

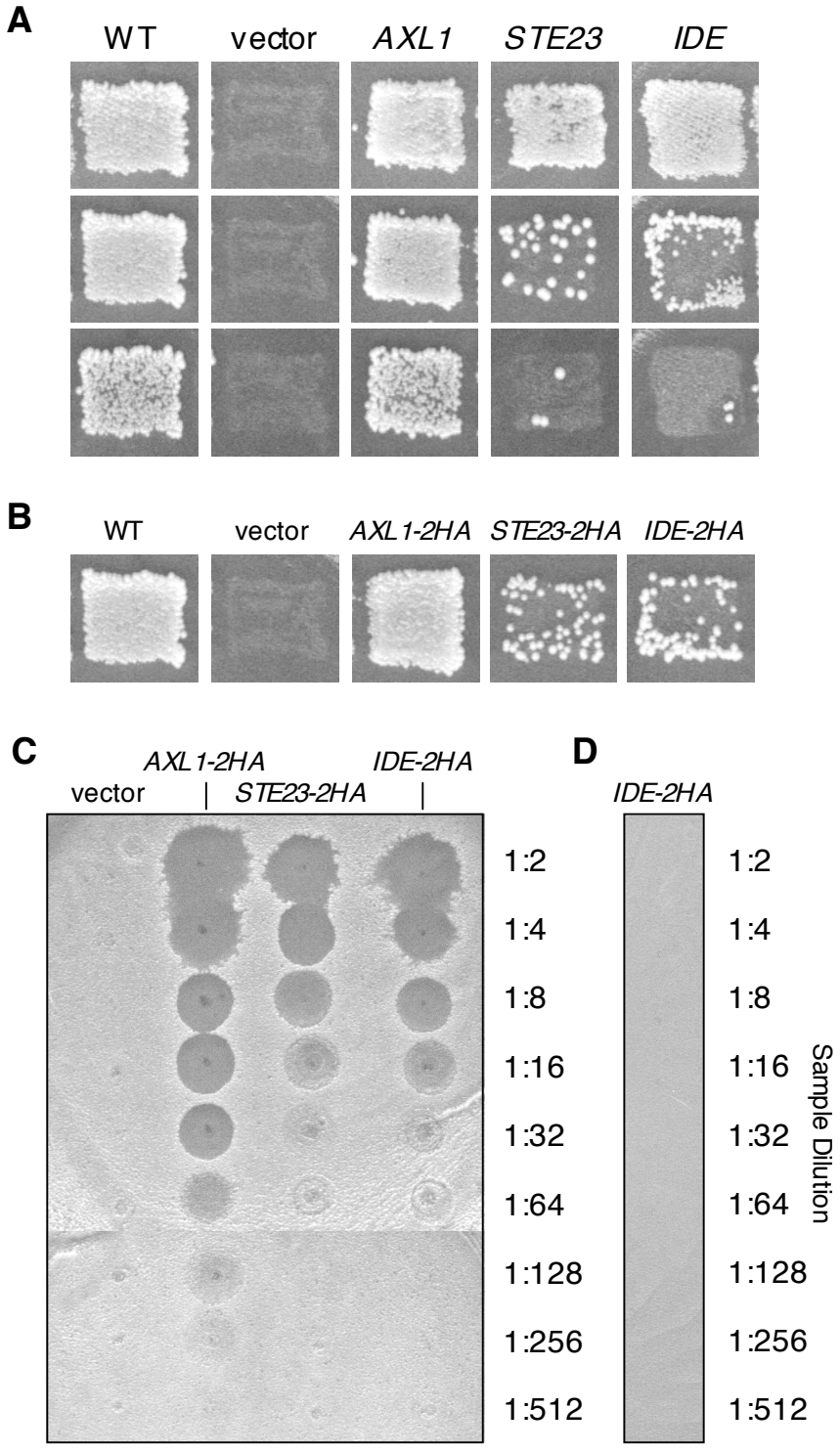
A
WT
vector
AXL1
STE23
IDE
B
WT
vector
AXL1-2HA
STE23-2HA
IDE-2HA
C
AXL1-2HA
IDE-2HA
vector
STE23-2HA
1:2
1:4
1:8
1:16
1:32
1:64
1:128
1:256
1:512
D
IDE-2HA
1:2
1:4
1:8
1:16
1:32
1:64
1:128
1:256
1:512
Sample Dilution

**Fig. 2.4.** *Mass spectroscopic analysis of* ***a****-factor produced by IDE, Ste23p, and Axl1p-expressing yeast strains.*

The **a**-factor species secreted by the indicated *MAT***a** strains were enriched from conditioned media as described in Fig. 2.3C, and samples were subjected to MALD-TOF/TOF mass spectroscopy using α-cyano-4-hydroxycinnamic acid as the matrix. The strains used were Y272 transformed with pWS496 (*IDE-2HA*), pWS482, (*STE23-2HA*), pWS372 (*AXL1-2HA*), or pRS316 (vector) (A-D, respectively). Deisotoping of the data shown in panels A-D resulted in the data presented in panels E-H, respectively. All strains also contained pSM463 (*2μ TRP1 MFA1*).

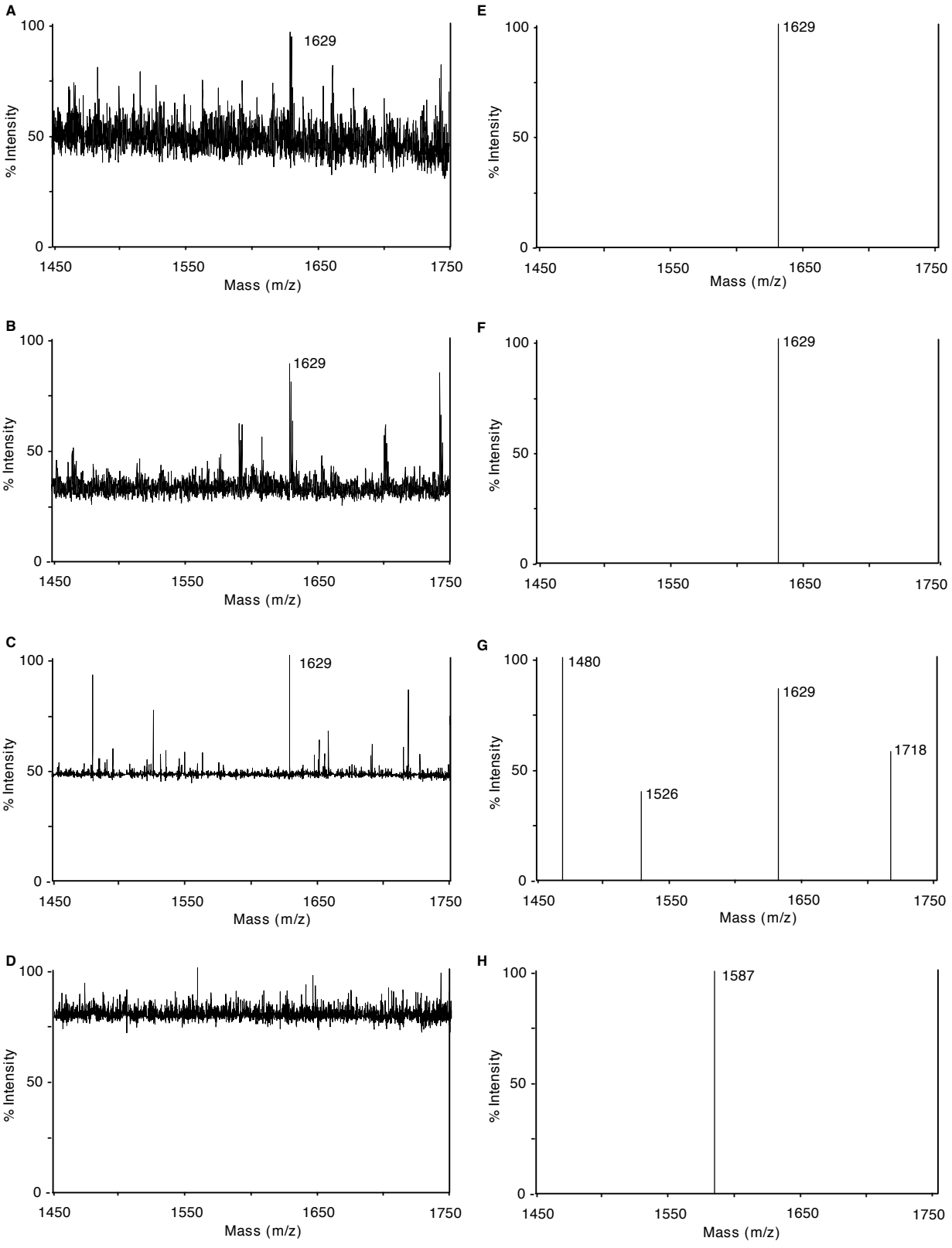
A
100
50
0
% Intensity
1629
1450
1550
1650
1750
Mass (m/z)
B
100
50
0
% Intensity
1629
1450
1550
1650
1750
Mass (m/z)
C
100
50
0
% Intensity
1629
1450
1550
1650
1750
Mass (m/z)
D
100
50
0
% Intensity
1450
1550
1650
1750
Mass (m/z)
E
100
50
0
% Intensity
1629
1450
1550
1650
1750
Mass (m/z)
F
100
50
0
% Intensity
1629
1450
1550
1650
1750
Mass (m/z)
G
100
50
0
% Intensity
1480
1629
1718
1526
1450
1550
1650
1750
Mass (m/z)
H
100
50
0
% Intensity
1587
1450
1550
1650
1750
Mass (m/z)

**Fig. 2.5.** *Evaluation of IDE, Ste23p, and Axl1p mutants.*

A-C) Alanine-substitution point mutations were created in IDE (A), Ste23p (B), and Axl1p (C), and the functions of the mutant enzymes were evaluated by patch mating tests as described in Fig. 2.3A under permissive conditions (100% YEPD). The mutations were created at sites invariably conserved between IDE, Ste23p, and Axl1p and include residues that comprise the extended metalloprotease motif of these enzymes ($HxxEHx_{69}Ex_6E$). The mutants exhibiting robust mating were as active as the unmodified parent enzyme as judged by mating tests under more stringent conditions.The strain used was Y272 transformed with IDE-encoding plasmids: pWS511 (*IDE-HA*), pWS531 (*IDE-HA* $H_{108}A$), pWS532 (*IDE-HA* $C_{110}A$), pWS533 (*IDE-HA* $E_{111}A$), pWS590 (*IDE-HA* $H_{112}A$), pWS591 (*IDE-HA* $E_{182}A$), pWS592 (*IDE-HA* $E_{189}A$), pWS572 (*IDE-HA* $C_{257}A$), pWS598 (*IDE-HA* $C_{414}A$), pWS599 (*IDE-HA* $C_{819}A$), pWS 573 (*IDE-HA* $S_{965}A$), pWS600 (*IDE-HA* $C_{110}A$, $C_{257}A$), Ste23p-encoding plasmids: pWS482 (*STE23-2HA*), pWS514 (*ste23-2HA* $H_{118}A$), pWS527 (*STE23-2HA* $C_{120}A$), pWS512 (*ste23-2HA* $E_{121}A$), pWS515 (*ste23-2HA* $H_{122}A$), pWS567 (*ste23-2HA* $E_{192}A$), pWS513 (*ste23-2HA* $E_{199}A$), pWS571 *(STE23-2HA* $C_{267}A$), and Axl1p-encoding plasmids: pWS371 (*AXL1-2HA*), pWS388 (*axl1-2HA* $H_{68}A$), pWS534 (*AXL1-2HA* $C_{70}A$), pWS389 (*axl1-2HA* $E_{71}A$), pWS390 (*axl1-2HA* $H_{72}A$), pWS391 (*AXL1-2HA* $E_{149}A$), pWS392 (*axl1-2HA* $E_{156}A$), pWS569 *(AXL1-2HA* $C_{224}A$), pWS568 (*AXL1-2HA* $S_{1081}A$).

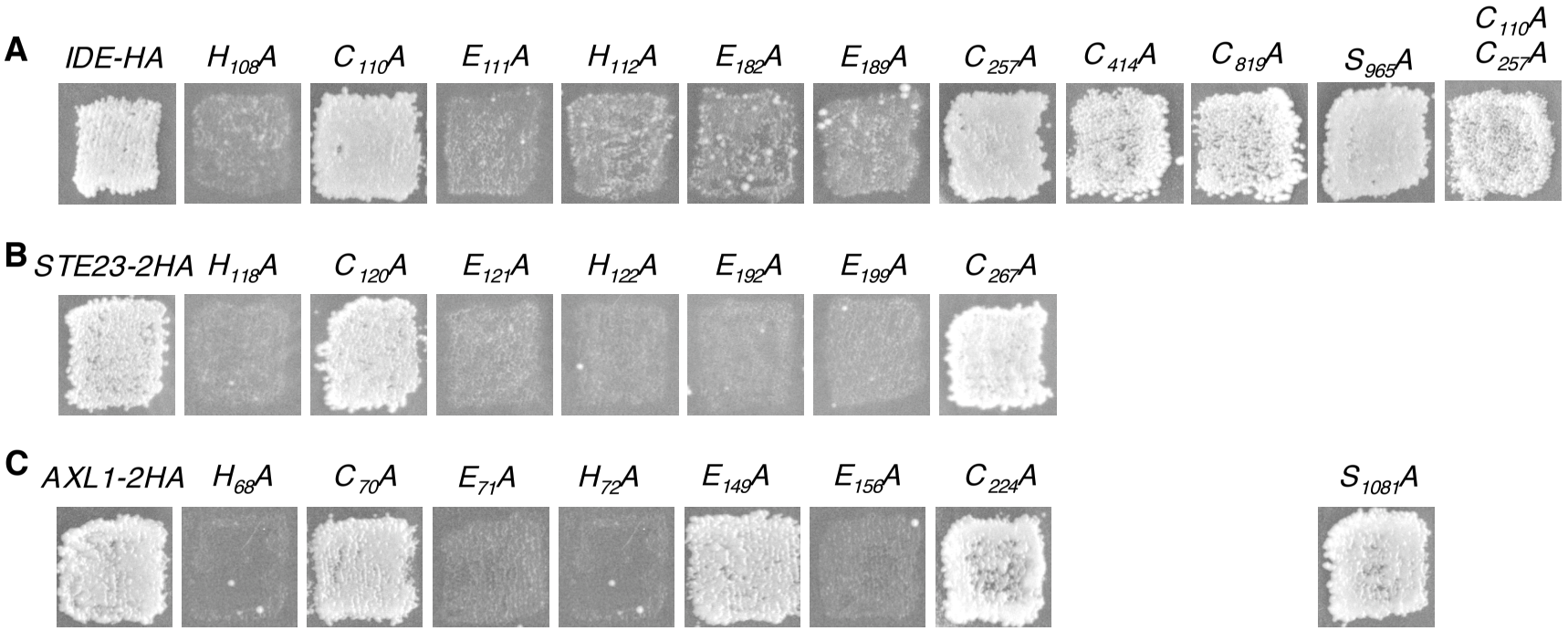
A
IDE-HA
H108A
C110A
E111A
H112A
E182A
E189A
C257A
C414A
C819A
S965A
C110A C257A
B
STE23-2HA
H118A
C120A
E121A
H122A
E192A
E199A
C267A
C
AXL1-2HA
H68A
C70A
E71A
H72A
E149A
E156A
C224A
S1081A

**Fig. 2.6.** *Evaluation of GFP-labeled IDE and Axl1p truncation mutants*

A) Full-length and C-terminally truncated versions of IDE and Axl1p were created as fusions to GFP, and the activities of these fusions were evaluated by patch mating tests under permissive conditions (100% YEPD). The truncations exhibiting robust mating were as active as the full-length fusion as judged by mating tests under stringent conditions, except for Axl1 1-1081 that had a reduced mating phenotype. The amino acids to which GFP was fused are indicated by the arrows and are shaded in gray. The residues within the C-terminal regions of IDE and Axl1p that are conserved are shown in the protein alignment below the mating tests (arrowheads). The residue in this region that was targeted for site-directed mutational analysis (see Fig. 2.5) is indicated (filled arrowhead). B) Protein extracts were prepared from yeast containing vectors encoding GFP-tagged IDE. Equivalent amounts of each sample were analyzed by SDS-PAGE and immunoblot using an anti-GFP antibody. The strain used was Y272 transformed with IDE-encoding plasmids: pWS539 (*IDE[1-960]-GFP*), pWS548 (*IDE[1-965]-GFP*), pWS549 (*IDE[1-968]-GFP*), pWS550 (*IDE[1-973]-GFP*), and pWS538 (*IDE[1-1019]-GFP*), and Axl1p-encoding plasmids: pWS551 (*axl1[1-1076]-GFP*), pWS541 (*AXL1[1-1081]-GFP*), pWS552 (*AXL1[1-1084]-GFP*) pWS553 (*AXL1[1-1089]-GFP*), pWS380 (*AXL1[1-1208]-GFP*).

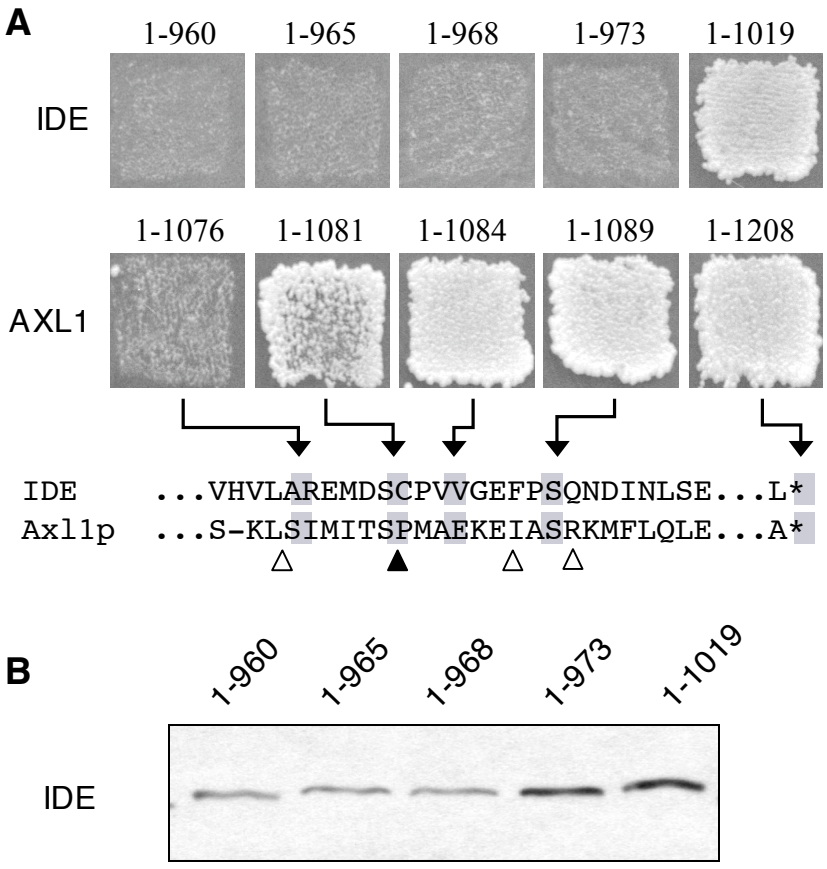
A
1-960
1-965
1-968
1-973
1-1019
IDE
1-1076
1-1081
1-1084
1-1089
1-1208
AXL1
IDE ...VHVLAREMDSCPVVGEFPSQNDINLSE...L*
Axl1p ...S-KLSIMITSPMAEKEIASRKMFLQLE...A*
B
1-960
1-965
1-968
1-973
1-1019
IDE

**Fig. 2.7.** *IDE cannot repress haploid invasive growth.*

Plasmids encoding HA-tagged Axl1p, Axl1p $H_{68}A$, and IDE were transformed into an *axl1* haploid strain. Equal cell density suspensions of these strains were spotted onto SC-ura and allowed to grow 4 days (A) after which the plates were washed with running water to remove surface lying cells (B). The presence of cells after the washing step is indicative of invasive growth. Strains used are Sy3687 transformed with pRS316 (WT), and Sy3721 (*axl1::HIS3*) transformed with: pRS316 (vector), pWS371 (*AXL1-2HA*), pWS388 (*axl1-2HA* $H_{68}A$), or pWS496 (*IDE-2HA*).

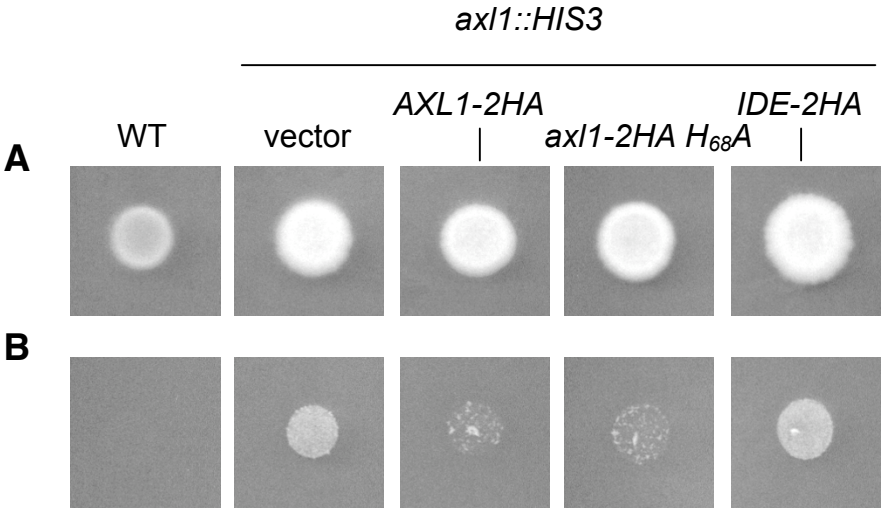
axl1::HIS3
AXL1-2HA
IDE-2HA
WT
vector
axl1-2HA H68A
A
B

**Fig. 2.8**. Schematic of M16A enzyme sequences.

A) The sequences of IDE, Ste23p, *E. coli* Protease III, and Axl1p are represented in cartoon format (top to bottom, respectively). The schematic has been drawn to scale. Each cartoon representation has been divided into several domains. The borders of domains I-VI are operationally defined as sites where insertions (>10 residues) are found in the Axl1p sequence as determined by multiple sequence alignment (ClustalW) of all four proteins. Domains at the ends of the molecules (horizontal stripes) represent sequences that are of variable length and not conserved between the enzymes. The N-terminal sequences range between 19 and 69 residues, and the C-terminal sequences range between 35 and 127 residues. The relative position of the shortest C-terminal truncation yielding a non-functional mutant is shown (filled arrowhead). The values below the schematic represent the percent identity between the indicated IDE domain and the corresponding domains of either Ste23p, *E. coli* Protease III, or Axl1p as determined using DNA Strider 1.3 at default settings. B-D) Several conserved motifs can be identified within domains I (B), II (C), and V (D). For the purposes of this figure, a conserved motif was defined as a block of amino acids (≥10) having ≥50% identical or highly conserved residues (*i.e.*, S/T, K/R, or A/I/V). The second motif listed for domain I is found within the $x_{69}$ sequence of the extended metalloprotease motif, while the third is found within the $x_{57}$ sequence. The residues in bold were mutated in this study. Neither $C_{257}$, which is found near the end of domain I (B), nor $C_{414}$, which is found at the beginning of domain IV, are within conserved motifs.

**A**

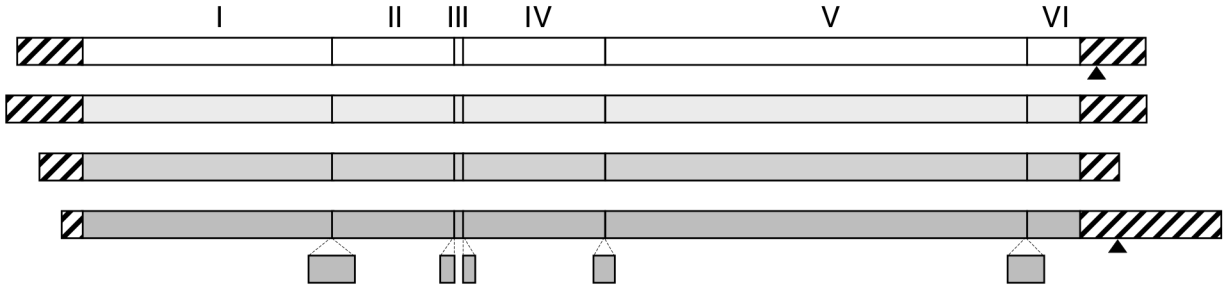


| | I | II | III | IV | V | VI |
|---|---|---|---|---|---|---|
| Ste23p | 56 | 42 | 38 | 38 | 33 | 23 |
| Protease III | 41 | 22 | 38 | 22 | 23 | 23 |
| Axl1p | 35 | 26 | 25 | 16 | 17 | 17 |

**B**

| | | | |
|---|---|---|---|
| IDE | DPPNIAGLS**H**FC**EH**$X_{69}$**E**$X_7$**E**$X_{57}$**C** | GSSNAFTSGEHT | HPFSKFGTGN |
| Ste23p | DPKNLPGLA**H**FC**EH**$X_{69}$**E**$X_7$**E**$X_{57}$**C** | GSSNAYTASQNT | HPYHKFSTGN |
| Protease III | DPEAYQGLA**H**YL**EH**$X_{69}$**E**$X_7$**E**$X_{57}$V | GSHNASTAPYRT | HPGSKFSGGN |
| Axl1p | DPKDIAGLA**H**LC**EH**$X_{76}$**E**$X_7$**E**$X_{57}$**C** | GSQNAFTTGEQT | HPFSRFSTGN |

**C**

| | |
|---|---|
| IDE | LIGHEGPGSL |
| Ste23p | LIGHEGSGSL |
| Protease III | LIGNRSPGTL |
| Axl1p | LFGDESPGSL |

**D**

| | |
|---|---|
| IDE | LRTKEQLGYIV |
| Ste23p | LRTKEQLGYVV |
| Protease III | LRTEEQLGYAV |
| Axl1p | LRNKKQIGYIV |

# CHAPTER 3

# DISCUSSION

During the development of the yeast system to study IDE function, we have made a number of additional observations. These are focused on the enzymatic properties of IDE and the potential utility of our system.

## 3.1. Proteolytic activity in the supernatant fraction

Although Axl1p and Ste23p were expressed and enriched in the particulate fraction, there was no insulin-degrading activity associated with this fraction. However, we found that Axl1p, Ste23p, and IDE were also found in the supernatant fraction (Fig. 3.1A). To evaluate the activity of the enzymes in this fraction, we used the previously described *in vitro* insulin degradation assay. Using the supernatant fraction as a source of the enzyme activity, we found that all three yeast-expressed enzymes in this fraction were able to cleave insulin *in vitro* (Fig. 3.1B). This data suggests that the localization of the enzymes may affect the proteolytic activity and that the enzymes in the supernatant fraction have different enzymatic properties. Several reports suggest the structural properties are important for the activity of IDE. For example, IDE exists as a mixture of dimers and tetramer, and the dimer is the more active form (1). Also, substrate binding to IDE is proposed to induce a conformational change associated with activation (2). Therefore, structural changes may be required for the activation of M16A enzymes. Whether Axl1p and Ste23p undergo structural changes has not been reported. The

enzymes in the particulate fraction could lack an ability to change conformation because they are tightly associated with membrane proteins or macromolecules of the particulate fraction, whereas the soluble forms of enzymes may be more flexible to alter their structure. IDE is not an endogenous enzyme in yeast, thus it may be more loosely associated with other proteins or molecules in the particulate fraction by comparison to Axl1p and Ste23p. Further investigation into the relationship between the localization and activity of the enzymes is warranted.

### 3.2. Structural importance of semi-conserved cysteines

We have found that there is higher insulin degrading activity for certain cysteine mutations of IDE (Fig. 3.2). As noted previously, IDE is sensitive to sulfhydryl modifiers, thus cysteine residues in IDE are believed to be important for its activity. We identified several conserved cysteines between yeast enzymes and IDE, created mutations of these conserved cysteine residues ($C_{110}A$ and $C_{257}A$) in IDE, and evaluated the sensitivity of the mutants to inhibitors. In this study, we found that Cys-110 and Cys-257 were not the targets of inhibitors. Interestingly, these mutations had slightly higher activity rather than wild type IDE. Two possibilities could explain these results. First, these cysteine residues may be involved in the formation of the dimer or tetramer forms of IDE than its catalytic activity, because different forms of IDE have different properties and activities (3). Second, these resides may be important for interaction with cellular factors that inhibit activity. Such putative inhibitors have not been definitively identified (4,5). However, we would not expect these inhibitory factors to endogenously exist in yeast. Nevertheless, our preliminary observation will lead us to investigate whether these novel alleles of IDE have increased activity.

### 3.3. Investigation of substrate specificity using yeast system

Inappropriate proteolytic activity can result in biological problems, and is the cause of many human diseases, such as Alzheimer disease. Thus, research on proteases often focuses on identifying the target substrates and inhibitors of various proteases with the final goal of developing treatments. The first step in identifying the substrates and inhibitors of a protease is understanding its substrate specificity. The substrate specificity of IDE has not been determined. Several studies report that its specificity may depend on primary amino-acid sequence, while others propose that substrate recognition depends on the secondary or tertiary structure (3,6,7). Unfortunately, a three-dimensional model of IDE is not available, and therefore, its interactions with substrates are not well understood. If the substrate specificity of IDE is governed by the primary sequence of its substrate, P and P′ subsites should influence its activity. P subsites are amino acids on N-terminal side of the cleavage site where $P_1$ is the first amino acid on N-terminal side of the cleavage site. P′ sites are oriented toward the C-terminus; thus $P_1'$ is the first amino acid on the C-terminal sides of the cleavage site. $P_1$-$P_1'$ is the bond that is cleaved in the substrate.

Our genetic system is ideal for investigating the substrate specificity of IDE. To do this, we will take advantage of yeast mating as a reporter system. $P_1$, $P_2$, and $P_3$ amino acids in the **a**-factor precursor will be mutated, and the effects of these mutations on the enzymatic activity of IDE will be evaluated as an indirect measure of cleavage. P′ sites will not be evaluated because these mutations would be expected to alter the biological activity of **a**-factor (8). Toward our goal, a collection of P subsite **a**-factor mutations has been created and is awaiting evaluation. We expect that this pool of **a**-factor mutants will be used to evaluate the substrate specificity of

Axl1p and Ste23p to further our understanding of the conserved enzymatic properties between M16A proteases.

### 3.4. Another approach to study proteolytic activity of M16A proteases

Protein aggregation is an important process in several neurodegenerative diseases, including Alzheimer disease, mad-cow disease, and others. In many cases, these aggregates possess characteristics of amyloid formation (9). Yeast prion [*PSI*$^+$], the translation termination factor Sup35p, has been used as a model to the study cellular mechanisms of prion development (10). The aggregation of Sup35p induces a loss of function for this protein and eventually leads to translation termination defects that comprise the [*PSI*$^+$] phenotype (11). Yeast Sup35p consists of three domains. First, Sup35N is a N-terminal domain that is responsible for prion formation. Second, Sup35C is a C-terminal domain that is required for translation termination. Third, Sup35M is located between Sup35C and Sup35N (10). Recently, the research group of Dr. Lynn at Emory University has reported that replacing the Sup35N domain with the Aβ sequence dose not disrupt the [*PSI*$^+$] phenotype (personal communication). Therefore, Sup35p Aβ has the same ability to aggregate in yeast. We hypothesize that Sup35p Aβ can serve as a substrate for IDE and/or the yeast proteases Axl1p and Ste23p, which will allow us to evaluate their activity to cleave Aβ *in vivo*. Furthermore, we can use this system to evaluate the proteolytic activity of M16A metalloprotease family. Based on our hypothesis, M16A metalloproteases will cleave Sup35p Aβ to prevent aggregation and repress the [*PSI*$^+$] phenotype.

### 3.5. Application of our system for the study of *E. coli* Protease III

*E. coli* Protease III is another member of M16A metalloprotease family that is also capable of cleaving insulin (12). Like IDE, we have hypothesized that Protease III may share enzymatic properties with Axl1p and Ste23p in promoting yeast mating. We have recently

determined that Protease III can indeed cleave the **a**-factor procursor peptide and promote yeast mating *in vivo* (Benjamin Alper, unpublished observations). Therefore, we conclude that the **a**-factor precursor can be used as a common substrate for the M16A metalloprotease family.

**Conclusion**: We first hypothesized that IDE could substitute for the proteolytic function of yeast proteases involved in **a**-factor production. By confirming our hypothesis, we have established that the proteolytic activity of the enzymes appears to be conserved. Thus, we propose that yeast is a suitable genetic model system for the study of IDE function and very likely that of Protease III. Our system is the first genetically tractable system for the study of these rather uncharacterized members of the M16A enzymes. In the future, we expect to use our system to probe the enzymatic properties of IDE and to investigate the substrate specificity of this enzyme. Also, we expect to investigate the hypothesis that M16A enzymes have a preference to cleave amyloid forming proteins. This line of investigation may yield novel alleles of IDE that have enhanced Aβ cleaving activity that may be therapeutic value.

### 3.6. References


1. Song, E. S., Juliano, M. A., Juliano, L., and Hersh, L. B. (2003) *J Biol Chem* **278**(50), 49789-49794
2. Kurochkin, I. V. (2001) *Trends Biochem Sci* **26**(7), 421-425
3. Duckworth, W. C., Bennett, R. G., and Hamel, F. G. (1998) *Endocr Rev* **19**(5), 608-624
4. Ogawa, W., Shii, K., Yonezawa, K., Baba, S., and Yokono, K. (1992) *J Biol Chem* **267**(2), 1310-1316
5. Ryan, M. P., and Duckworth, W. C. (1983) *Biochem Biophys Res Commun* **116**(1), 195-203
6. Authier, F., Posner, B. I., and Bergeron, J. J. (1996) *Clin Invest Med* **19**(3), 149-160
7. Song, E. S., Mukherjee, A., Juliano, M. A., Pyrek, J. S., Goodman, J. P., Jr., Juliano, L., and Hersh, L. B. (2001) *J Biol Chem* **276**(2), 1152-1155
8. Caldwell, G. A., Wang, S. H., Xue, C. B., Jiang, Y., Lu, H. F., Naider, F., and Becker, J. M. (1994) *J Biol Chem* **269**(31), 19817-19825
9. Koo, E. H., Lansbury, P. T., Jr., and Kelly, J. W. (1999) *Proc Natl Acad Sci U S A* **96**(18), 9989-9990
10. Chernoff, Y. O. (2001) *Mutat Res* **488**(1), 39-64
11. Chernoff, Y. O., Derkach, I. L., and Inge-Vechtomov, S. G. (1993) *Curr Genet* **24**(3), 268-270
12. Ding, L., Becker, A. B., Suzuki, A., and Roth, R. A. (1992) *J Biol Chem* **267**(4), 2414-2420

**Fig. 3.1.** *Axl1p, Ste23p, and IDE in supernatant fractions can cleave insulin in vitro.*

A) A total lysate containing HA-tagged Axl1p, Ste23p, and IDE was subjected to differential centrifugation at 13,000g. Corresponding particulate (P) and supernatant (S) fractions were recovered and equivalent amounts of protein (10μg) were analyzed by SDS-PAGE and immunoblotting with the HA monoclonal antibody. B) Particulate (P) and supernatant (S) fractions were isolated from yeast expressing Axl1p, Ste23p, or IDE. An equivalent amount of each fraction (5μg) was assayed for insulin degradation activity for the t=0 min and t=120 min. The degradation of insulin is indicated by the presence of recovered insulin fragments that cannot be precipitated by TCA.

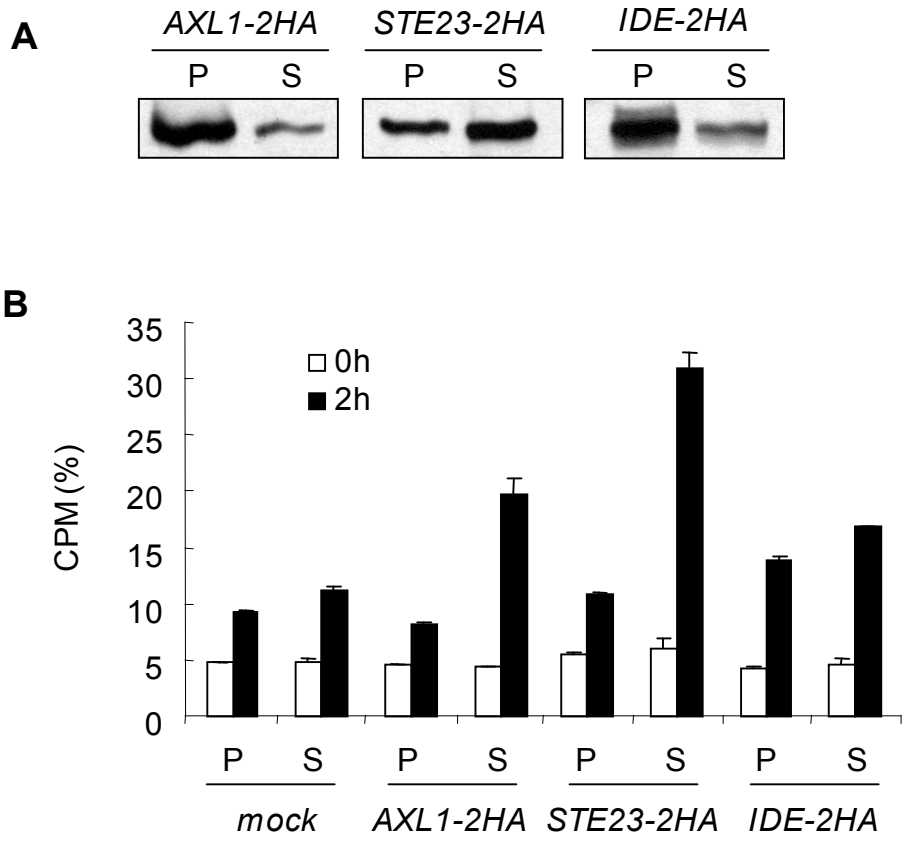
A
AXL1-2HA
STE23-2HA
IDE-2HA
P
S
P
S
P
S
B
CPM (%)
35
30
25
20
15
10
5
0
0h
2h
P
S
P
S
P
S
P
S
mock
AXL1-2HA
STE23-2HA
IDE-2HA

**Fig. 3.2.** *Cysteine mutations of IDE have higher activity for insulin degradation.*

Particulate fractions were isolated from yeast expressing IDE, IDE $C_{110}A$, IDE $C_{257}A$, and IDE $C_{110}A/C_{257}A$. An equivalent amount of each fraction (5μg) was assayed for insulin degradation activity for the t=0 min and t=120 min.

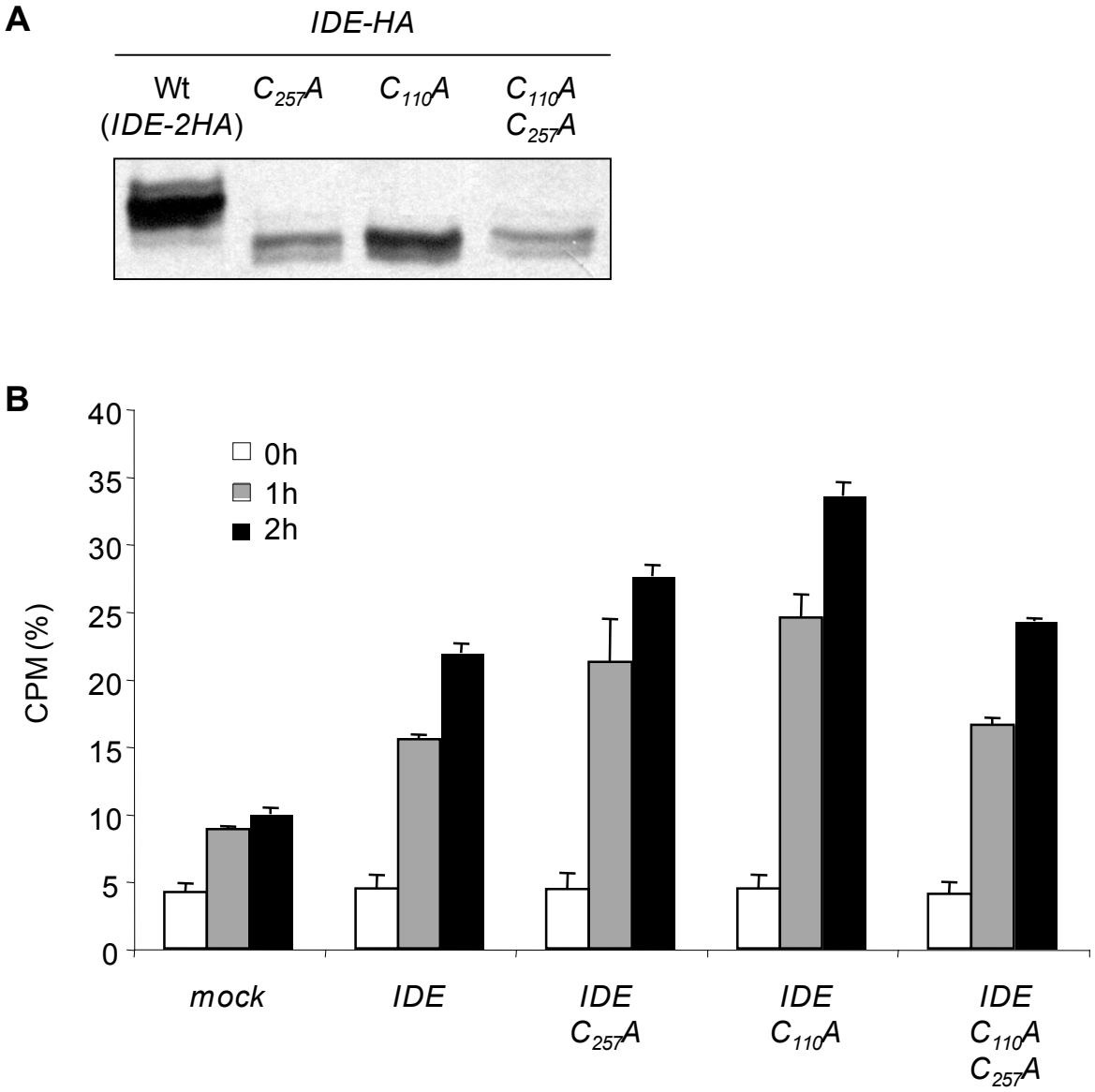
A
IDE-HA
Wt
(IDE-2HA)
C257A
C110A
C110A
C257A
B
CPM (%)
0h
1h
2h
0
5
10
15
20
25
30
35
40
mock
IDE
IDE
C257A
IDE
C110A
IDE
C110A
C257A